JIPB Journal of Integrative Plant Biology

Plant xylem hydraulics: What we understand, current research, and future challenges[FA]

Martin D. Venturas[1]*, John S. Sperry[1] and Uwe G. Hacke[2]

1. Department of Biology, University of Utah, 257 S 1400E, Salt Lake City, UT 84112, USA
2. Department of Renewable Resources, University of Alberta, Edmonton, AB T6G 2E3, Canada

doi: 10.1111/jipb.12534

Martin D. Venturas
*Correspondence:
martin.venturas@utah.edu

Abstract Herein we review the current state-of-the-art of plant hydraulics in the context of plant physiology, ecology, and evolution, focusing on current and future research opportunities. We explain the physics of water transport in plants and the limits of this transport system, highlighting the relationships between xylem structure and function. We describe the great variety of techniques existing for evaluating xylem resistance to cavitation. We address several methodological issues and their connection with current debates on conduit refilling and exponentially shaped vulnerability curves. We analyze the trade-offs existing between water transport safety and efficiency. We also stress how little information is available on molecular biology of cavitation and the potential role of aquaporins in conduit refilling. Finally, we draw attention to how plant hydraulic traits can be used for modeling stomatal responses to environmental variables and climate change, including drought mortality.

Edited by: William J. Lucas, University of California, Davis, USA
Received Jan. 10, 2017; **Accepted** Mar. 9, 2017; **Online on** Mar. 14, 2017
FA: Free Access, paid by JIPB

INTRODUCTION

Plants require large amounts of water to live and grow. Photosynthesis itself consumes one molecule of water for each molecule of CO_2 fixed. However, for each water molecule used in photosynthesis, hundreds more are lost by transpiration through stomata, which must be open to uptake CO_2. As a result, the water use efficiency (WUE) of plants, defined as the ratio between the rate of CO_2 assimilated and H_2O transpired by the plant, is very low and ranges between 0.5–10 mmol CO_2 (mol $H_2O)^{-1}$ (Nobel 1991). Ninety percent of trees with an average height of 21 m have maximum transpiration rates between 10 and 200 L of water per day (Wullschleger et al. 1998). A large overstory Amazonian rainforest tree can use up to 1,180 L of water per day (Jordan and Kline 1977). Such is the amount of water transpired by plants that across ecosystems transpiration returns an average of 39% of incident rain back to the atmosphere and, therefore, is an important factor in the global water cycle (Schlesinger and Jasechko 2014).

Vascular plants have evolved a highly specialized vascular tissue, the xylem, which exploits a passive, physical mechanism for supplying these large amounts of water to the photosynthetic organs (Sperry 2003; Lucas et al. 2013). No metabolic energy is used to generate the driving force for fluid flow, and the xylem conduits that carry the transpiration stream are dead cell wall skeletons. Indeed, the low WUE of plants would make an active transport mechanism unsustainable by creating a negative energy balance. Despite being a passive, physical process that occurs in dead cells, vascular water transport has been termed the "backbone of plant physiology" (Brodribb 2009), and the field of "plant hydraulics" has emerged as an increasingly dominant arm of plant water relations research.

In this review we highlight current research in plant hydraulics in the context of plant physiology, ecology, and evolution. We address methodological issues, and focus on current and future research opportunities. However, we first explain the physics of xylem water transport in plants and the limits of the system. Though simple, the transport mechanism and its relation to xylem anatomy is easily misunderstood.

PHYSICS AND ANATOMY OF WATER TRANSPORT IN PLANTS

The ascent of sap in plants is explained by the "cohesion-tension" theory (Dixon and Joly 1895; Pickard 1981). Details on the origin and the development of this theory were reviewed by Brown (2013). The conceptual basis of this theory is simple: Water molecules that evaporate from the leaves are replaced by others in the upstream liquid phase, which are pulled up the plant by capillary forces (Figure 1). These forces arise at air-water menisci formed between the apoplastic water in the pores of mesophyll cell walls and the intercellular air space (Figure 1B–E). Consider first the stationary situation where there is no transpiration, and gravity is the only external force acting on the meniscus. Each meniscus is anchored to the cell wall surface by the adhesion of liquid water to the hydrophilic wall via hydrogen bonding. Hydrogen bonding also creates the surface tension, which suspends the free surface of the meniscus against gravity. These capillary forces in the meniscus create a negative (sub-atmospheric) liquid pressure throughout the bulk fluid and balance the gravitational force. When transpiration is added to this situation, water evaporates from the meniscus whose edges remain firmly anchored by adhesion. The consequent tendency for the meniscus to increase its concavity and "sag" is resisted by surface tension, which holds the surface taut. The pull of surface tension on the meniscus is communicated to the bulk liquid, which experiences a further drop in pressure, which pulls water against frictional resistance through the continuous liquid phase flow path in cells and xylem conduits from the soil. Using an analogy with solids, the liquid water column acts like a rope under "tension" created by the "cohesion" of hydrogen-bonding properties that create capillary force. The "tension" term is by analogy because it is a directionally-dependent tensor quantity descriptive of forces acting on solids or surfaces, whereas forces in bulk liquid phase act as pressure: a scalar quantity which is directionally independent. These forces balance gravity, friction, and the capillary forces at the soil end of the hydraulic "rope", which resist drainage of the soil pore space (Figure 1A).

The cohesion-tension mechanism requires significantly negative pressures to operate. Gravitational force is generally the smallest contributor to the pressure gradient generated within the xylem, resulting in a pressure drop of approximately $-0.01\,\mathrm{MPa}\ \mathrm{m}^{-1}$ (e.g., $-0.3\,\mathrm{MPa}$ in a 30 m tall tree; Figure 2). The most important factor is the soil water potential, because the plant cannot have a xylem pressure that is above the water potential of its active rooting zone. The xylem sap pressure (P_x) must be lower or equal to the total soil water potential ($P_x \leq$ osmotic + pressure + matric components) because the incoming water is filtered through cell membranes at the root endodermis and in some cases at other points in the root (Steudle 2000). Typical soil water potentials that allow plant survival range from 0 in wet soils to below $-10\,\mathrm{MPa}$ in dry or very saline soils. The lowest xylem pressures are generally found in plants rooted in dry or saline soils, and reach approximately $-14\,\mathrm{MPa}$ (Jacobsen et al. 2007; Venturas et al. 2016a). The final contributing factor to xylem pressure is friction, which requires a steady-state pressure drop equal to the transpiration rate (E) divided by the hydraulic conductance of the soil-to-leaf flow path (k). The frictional pressure drop is typically between 1 and 2 MPa in trees under wet soil and dry air conditions that maximize E. Herbs generally experience somewhat smaller pressure drops. The frictional pressure drop is the one component of xylem pressure gradient that plants can actively influence via stomatal control of E at short term time scales (Figure 2). Stomata typically close partially in drier air to limit E and the associated pressure drop. This closure is accentuated in dry soil. In extreme soil drought, stomata are likely to close completely.

The xylem functions as a pathway of high hydraulic conductance that minimizes the frictional pressure drop

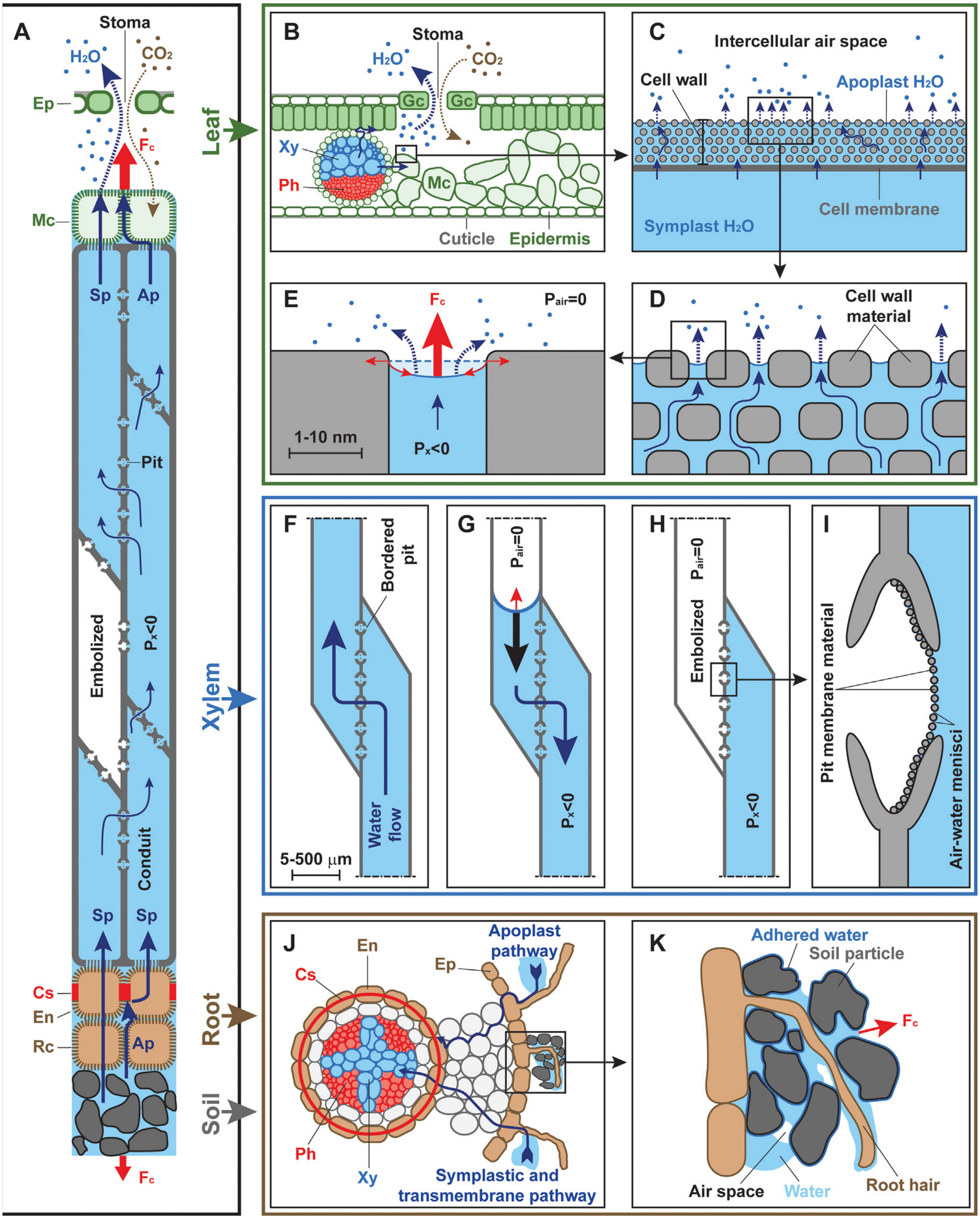

Figure 1. Cohesion-tension mechanism of ascent of sap in plants

(A) Schematic water column from soil to leaf cells (adapted from Sperry 2011). Liquid water is pulled (solid blue arrows) from the soil to the evaporating surface of leaf cell walls by negative water pressure ($P_x < 0$) created by cell wall capillary forces (red F_c arrow). This force moves water through the mesophyll (Mc) from the xylem via a symplastic and transmembrane pathway (Sp), an apoplastic pathway (Ap), or a combination of both. Water moves up the xylem through a network of conduits that must be full of water to function (not gas-filled or "*embolized*"). Water moves through root cells (Rc) from soil to root xylem via Ap and Sp pathways except where it is filtered at the endodermis (En) because the casparian strip (Cs) blocks the apoplastic pathway. The epidermis (Ep) and stomata control H_2O vapor loss (broken blue arrow) and CO_2 uptake (broken brown arrow) by diffusion from higher to lower partial pressures. **(B)** Leaf cross section, showing that the rate of evaporation from leaf cell walls (and hence potential for CO_2 uptake) is largely controlled by stomatal guard cell (Gc) aperture. **(C)** The evaporating surface of the leaf cell wall. **(D)** The air-water menisci held by surface tension and hydrophilic cell wall material. **(E)** Close up of a single meniscus illustrating the origin of the capillary pulling force (F_c). Adhesion of water to the wall (horizontal red arrows) anchors the meniscus edges. Evaporation (dashed blue arrows) causes the meniscus to retreat, increasing its curved surface area (curved meniscus surface relative to flat dashed surface). Surface tension resists the curvature, pulling the meniscus back to its equilibrium surface (dashed blue line), thereby exerting a pulling force that lowers the liquid pressure behind the meniscus ($P_x < 0$). This force is propaged through the continuum in **(A)**, moving water up from the soil. **(F)** Conduits in the xylem are connected to each other through pits which offer resistance to flow but provide safety to the system. **(G)** If air gets into these conduits, capillary forces are not strong enough to retain the water column because conduit diameters are too large, and **(H)** water recedes into the adjacent tissue and the vessel becomes embolized and non functional to water transport. **(I)** Pit "membranes" of modified primary cell wall material avoid the spread of air throughout the xylem network by generating the same capillary forces as the menisci of mesophyll cell walls. **(J)** Root cross section detailing water flow from soil to root xylem. The endodermis (En) with its casparian strip (Cs) interrupts apoplastic flow, forcing water through the En cell membranes by reverse osmosis. **(K)** Detail of water held in the soil by the same capillary forces that pull the water up the plant. Cohesion-tension is a tug of war on a rope of water by capillary forces in leaf vs. soil.

from the finest absorbing roots to the vein endings in leaves. The mature xylem conduits are dead and hollow, eliminating the obstacles of cell membranes and protoplasts. They are wide (approximately 5–500 μm in diameter) and long (mm to m) to minimize flow resistance, and their walls are lignified and with thick secondary walls to withstand collapse by their internally negative pressure (Hacke et al. 2001a; Sperry et al. 2006). The ancestral tracheid type of conduit develops from a single cell and is limited to generally less than a cm in length (rarely longer), whereas the derived vessel of angiosperms and certain other groups develops from a coordinated chain of cells (vessel elements) which partially or wholly lose their common end-walls (perforation plates). Vessels can be many cm to m in length (Zimmermann 1983; Jacobsen et al. 2012). Xylem conduits of either type are connected to each other by pits in the secondary cell wall that have a pit "*membrane*" separating the conduit lumens (Figures 1F–I, 3). This is not a cell membrane (the mature conduits are dead), but rather the modified primary cell walls and intervening middle lamella of the adjacent conduit cells. As will shortly be seen, although pit membranes create flow resistance, they play a crucial role in xylem transport safety.

Xylem conduits are "born" full of water, and they must stay full to function in carrying the transpiration stream. If they become gas filled, they are much too wide in diameter to hold an air-water meniscus against typical negative water pressures in xylem. The most negative pressure that a meniscus can generate ($P_{\min}$, Pa, relative to atmospheric) in a cylindrical capillary is determined by:

$$P_{\min} = -\frac{4\,\Gamma\cos(\theta)}{D_c} \tag{1}$$

where Γ is the surface tension ($N\,m^{-1}$), θ is the contact angle between the liquid and surface of the capillary (a measure of adhesion), and D_c is the capillary diameter (m). The negative symbol indicates that water pressure is subatmospheric. If pressure drops below $P_{\min}$ "capillary failure" occurs and the liquid column recedes. Cellulose and hemicelluloses microfibers (the main cell wall components) are hydrophilic components with small θ (<60 degrees) and pores ranging 1–10 nm. Sap Γ is usually considered to be equal to that of pure water Γ (Christensen-Dalsgaard et al. 2011). As at 20 °C water Γ is $0.07275\,N\,m^{-1}$ (Vargaftik et al. 1983), if we considered a $\theta = 60$ degrees, typical cell wall pores can generate a $P_{\min}$ of -14.5 to -145.5 MPa (for 10 and 1 nm, respectively). In contrast, typical lumen diameters of xylem conduits range from 5 to 500 μm; therefore, a gas-water meniscus spanning a xylem conduit would only be able to withstand xylem water pressures above -0.03 MPa for the narrower conduits ($-2.9 \cdot 10^{-4}$ MPa for the wider ones; gas pressure $P_a = 0$ MPa). As xylem pressures are typically more negative than -0.03 MPa capillary force generated in the conduit

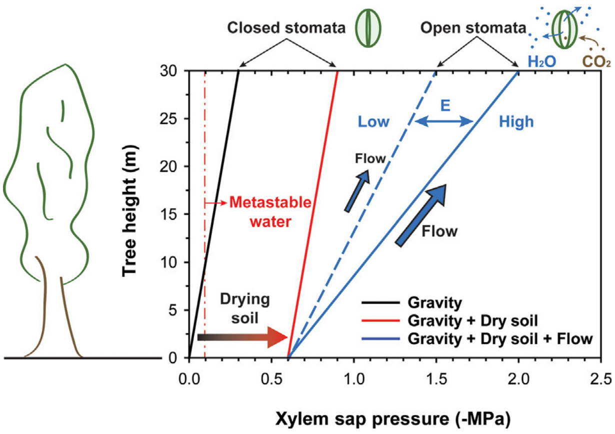

Figure 2. Pressure gradients in a tree

When soil is fully hydrated and stomata are closed the pressure gradient of the stationary, hanging water column balances gravitational force (black line). As soil dries the starting point of the pressure gradient is more negative but the slope is unchanged as long as there is no flow (red line). When plants open their stomata the slope of the pressure gradient within the plant increases due to friction (solid blue line) and transpiration (*E*) is proportional to the plant's hydraulic conductance and its soil to leaf pressure drop. Plants can actively control this frictional pressure drop by adjusting their stomatal aperture to vary *E* (e.g., the dashed blue line is the pressure drop for Low *E* whereas the solid blue line for High E). Water is transported in a metastable liquid state because the boiling point is only −0.099 MPa (red dash-dot line, assuming 101.3 kPa atmospheric pressure and 20 °C temperature). The metastable liquid realm is reached by the gravity gradient alone at $>$10 m height for plants in wet soil.

cannot hold the meniscus and water would drain out of the conduit (Figure 1F–I). These simple calculations indicate that the capillary force required for the cohesion-tension mechanism is generated in the mesophyll cell walls and *not* in xylem conduits. One role of the pit membranes between conduits is to serve as a capillary safety valve. The nanometer scale pores in the membrane are generally sufficient to arrest the air-water interface and prevent air from propagating easily between conduits (Figures 1I, 3). Plants could not survive long without pit membranes, because without them a single injury to the vascular system could completely disrupt transport.

The extra-xylary portion of the transpiration stream in roots and leaf mesophyll is extremely short ($<$1 mm), and much less obviously specialized for transport (Taiz and Zeiger 2010). As such, its relatively high resistance to flow can appreciably influence the plant's hydraulic conductance. In living tissues, the water travels either via an apoplastic pathway (i.e., flowing through cell walls and intercellular spaces), symplastic and transmembrane pathway (i.e., entering and exiting the cells flowing through plasmodesmata and cell membranes), or a combination of both (Figure 1; Steudle 2000). However, when water reaches the endodermis in the root, the apoplastic pathway is blocked by the casparian strip, forcing water to cross cell membranes (Figure 1J). This limits pathogen entry and controls solute uptake. During transpiration the flow through the endodermis cell membrane is pressure driven, but when soil moisture is high and no transpiration occurs, water can be taken up by osmosis creating positive xylem pressure (root pressure) (Steudle 2000). An endodermis may also be present in leaf tissue (Lersten 1997; Sack et al. 2015).

LIMITS TO THE COHESION-TENSION MECHANISM

Water at 20 °C boils at an absolute pressure of 2.3 kPa (Haynes 2014). Thus, relative to an atmospheric pressure of 101.3 kPa water should boil at −99 kPa (−0.0099 MPa relative to zero atmospheric pressure). Even in wet soil and with no transpiration, this negative pressure is induced by the gravity itself at 10 m in a tall tree (Figure 2). Trees can grow much taller than 10 m, with *Sequoia sempervirens* topping out over 100 m and requiring a gravitational pressure drop of below −1 MPa (Koch et al. 2004). But even short plants reach pressures well below −1 MPa because of dry soil and the frictional pressure drop (e.g., Jacobsen et al. 2007; Venturas et al. 2016a). Obviously for the cohesion-tension mechanism to work, boiling must be avoided, and hence the xylem water must enter a metastable liquid phase. Although this requirement has excited periodic dissent, the theory and evidence for metastable liquid water in plants and other systems is extensive (e.g., Zheng et al. 1991; Poole et al. 1992; Mishima and Stanley 1998; Wheeler and Stroock 2008). When referring to "negative pressure" it is important to emphasize that it refers to the *liquid* phase, because a negative *gas* phase pressure (i.e., below pure vacuum at zero molecular density) is indeed physically impossible. In liquid phase, molecular density obviously changes little with pressure, hence the analogy of a liquid under negative pressure with a solid under tension.

How is metastable liquid water possible? Boiling is typically triggered at nucleation sites, such as small air bubbles, impurities, and irregular contact zones that destabilize the hydrogen bonds among water molecules (Pickard 1981). Elimination of such nucleation sites in the xylem (or any other system) inhibits the phase change, and allows the metastable liquid phase to exist. A lower negative pressure limit exists where "cavitation" (the phase change from liquid to vapor) will occur by the spontaneous breaking of inter-molecular bonds even in an absolutely pure liquid. For pure water at physiological temperatures, this lower theoretical limit is below −30 MPa (Mercury and Shmulovich 2014), which is more negative than any xylem pressure measured in plants. Among the many experimental demonstrations of metastable liquid water are those of Briggs (1950), where liquid water sustained pressures down to −25 MPa (between 5 and 35 °C) within the central section of glass capillary tubes spinning in a centrifuge. Cavitation ultimately occurred, presumably triggered by irregularities in the contact between water and the glass wall.

Considerable research has elucidated the occurrence and mechanism of cavitation within the xylem conduits of plants. Cavitation in the liquid-filled conduit is accompanied by a rapid, but small, expansion of a gas void that immediately relaxes the negative sap pressure to near zero. This relatively high-pressure water is thereby released to be taken up by surrounding vascular tissue. As the conduit drains, the initially small gas void gradually grows to fill the entire conduit until it is arrested by the capillary action of the pit membranes (Figure 1H, I). A gas filled conduit constitutes an "embolism" that is non-transporting.

The air-seeding mechanism for drought-induced cavitation

The "air-seeding" hypothesis explains the mechanism by which xylem conduits become embolized under drought stress conditions (Zimmermann 1983; Crombie et al. 1985; Sperry and Tyree 1988). A functional xylem conduit (sap filled, $P_x < 0$) becomes air-seeded when it aspirates a gas bubble through a pit membrane connecting it to a neighboring conduit that is already gas filled ($P_a = 0$; Figures 4B). The gas bubble nucleates cavitation, and then gradually expands until the conduit becomes embolized as water recedes into adjacent tissue (Figure 1G). The pressure difference required to pull the air bubble through an idealized cylindrical pit membrane pore is given by the capillary equation (Eq. 1). It should be recognized, however, that the actual manner by which the gas leaks across the membrane is potentially quite complex (Schenk et al. 2015). It has also been suggested that organic surfactants could stabilize seeded bubbles and prevent them from immediately nucleating cavitation (Schenk et al. 2015, 2016), though direct evidence for this is lacking.

Air-seeding in conifers and angiosperms is slightly different due to their different pit membrane structure (Figures 3, 4B). Conifer pit membranes have two differentiated areas: the *torus*, the center circle that is very dense and has very small pores, and the *margo*, which is the external highly porous ring that has very low resistance to sap flow (Figure 3C; Hacke et al. 2004; Pittermann et al. 2005). When a conduit is embolized the membrane is deflected against the contiguous water filled one and the torus creates a seal with the pit border to avoid air spreading through the vascular system through the porous margo (Figure 4B). However, if the pressure difference is large enough, air seeding is thought to occur when air is pulled through the pit border-torus seal or a torus pore (Cochard et al. 2009; Delzon et al. 2010; Jansen et al. 2012; Bouche et al. 2014), or when the torus is displaced allowing air to seed through the large margo pores (Sperry and Tyree 1990; Hacke et al. 2004). Angiosperms have a more homogeneous pit membrane and therefore air-seeding occurs through the largest pore within the membrane (which may be a pre-existing pore, or one created during membrane displacement) or by membrane rupture (Figures 3B, 4B; Sperry and Tyree 1988). Air-seeding requires an embolized conduit to start with, but such are common owing to mechanical rupture of the vascular system. Leaf drop, root senescence, breakage from storms, fire, or herbivores, and even the endogenous rupture of elongating protoxylem during regular plant development will create embolized conduits that serve as initiators of the air-seeding process (Figure 4A).

Support for the air-seeding hypothesis has been obtained from several lines of evidence. One of the most compelling is the use of positive air pressure to induce embolism. The negative pressure P_x required for aspirating an air bubble through a pore of the

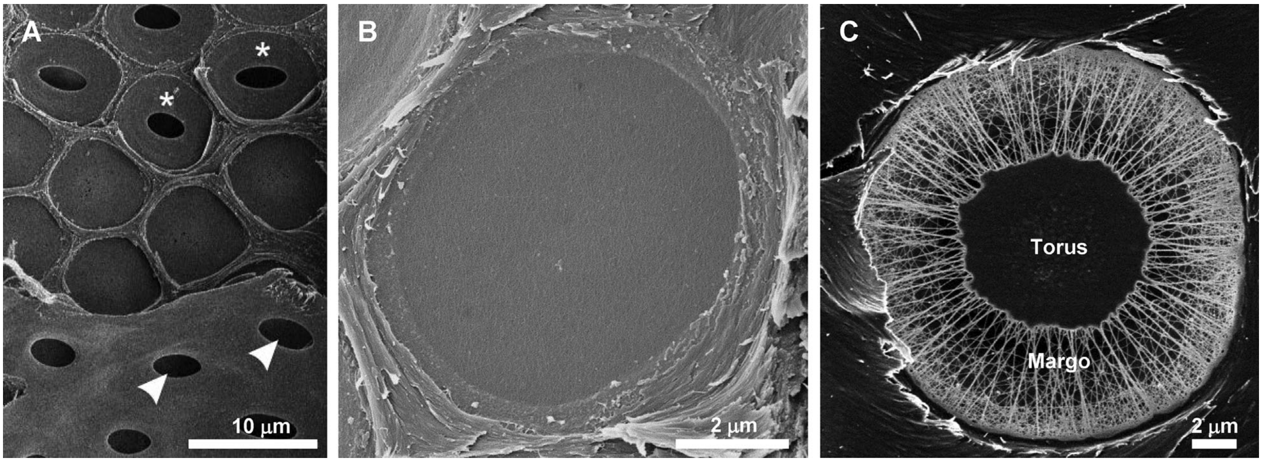

Figure 3. Interconduit pit field and pit membranes
(A) Inter-vessel pit field in a hybrid poplar stem (*Populus trichocarpa* × *deltoides*). The pits in the upper third of the image have their membranes removed (asterisks); the pits in the center have their membrane but the pit border facing the viewer is removed; the pits on the lower third of the image show the pit apertures from the other side of the vessel wall (arrow heads). Scale bar = 10 µm. Photograph: Lenka Plavcová. **(B)** Surface view of pit membrane of an angiosperm (*Acer platanoides*) with fairly small and homogeneous pores. Scale bar = 2 µm. Photograph: Brendan Choat. **(C)** Pit membrane of a conifer (*Picea glauca*) root tracheid showing the typical torus-margo structure. Scale bar =2 µm. Photograph: Amanda Schoonmaker.

intervessel pit membrane in theory should be equal to the positive pressure required to push a bubble through the same pore when $P_x = 0$, and these two values have been shown to be consistent (Lewis 1988; Sperry and Tyree 1988; Cochard et al. 1992; Sperry et al. 1996). Moreover, as indicated by Eq. 1, if surface tension is lower the pressure required to push air through the pit membrane pore is also lower, so the cavitation pressure should become less negative; this has also been confirmed by perfusing samples with solutions of different surface tension (Crombie et al. 1985; Sperry and Tyree 1988). Correlations have been obtained between mean cavitation pressures and pit membrane thickness and porosity estimated both by perfusing nanospheres (Jarbeau et al. 1995) and by analyzing scanning electron microscopy (SEM) and transmission electron microscopy (TEM) images (Jansen et al. 2009; Lens et al. 2010; Plavcová et al. 2011). However, seeding pressures often indicate larger pore sizes than those observed microscopically (e.g., Choat et al. 2003). A likely reason is that the single largest pore in the inter-conduit wall that actually causes the air-seeding could be an extremely rare outlier (Wheeler et al. 2005; Christman et al. 2009, 2012). Moreover pit membrane porosity may increase when the membrane is aspirated against the bordered pit wall (Figures 1I, 4B) due to the pressure difference between a gas and water filled conduit (Choat et al. 2003, 2004). Some angiosperms have vestured pits, which reduce the probability of the pit membrane being stretched and, therefore, protect the membrane from mechanical stress that can contribute to the air-seeding process (Choat et al. 2004). Spatial aggregation of embolized conduits shown with imaging techniques such as active xylem staining (Sperry and Tyree 1988) and high resolution X-ray computed tomography (HRCT; Choat et al. 2015; Torres-Ruiz et al. 2016) also provide strong evidence for the conduit-to-conduit spread of embolism predicted by the air-seeding hypothesis.

Freeze-thaw induced cavitation

Freeze-thaw cycles can also induce xylem embolism (Zimmermann 1983; Sperry and Sullivan 1992). According to the "thaw expansion hypothesis", as sap freezes, dissolved gasses are forced out of solution and form bubbles in the conduits. When the sap thaws these bubbles can either dissolve back into the sap or nucleate cavitation. If the latter happens the conduit becomes embolized and non-functional (Figure 4C). The main factors that determine if a gas bubble dissolves or not are the internal pressure (P_b) and diameter (D_b)

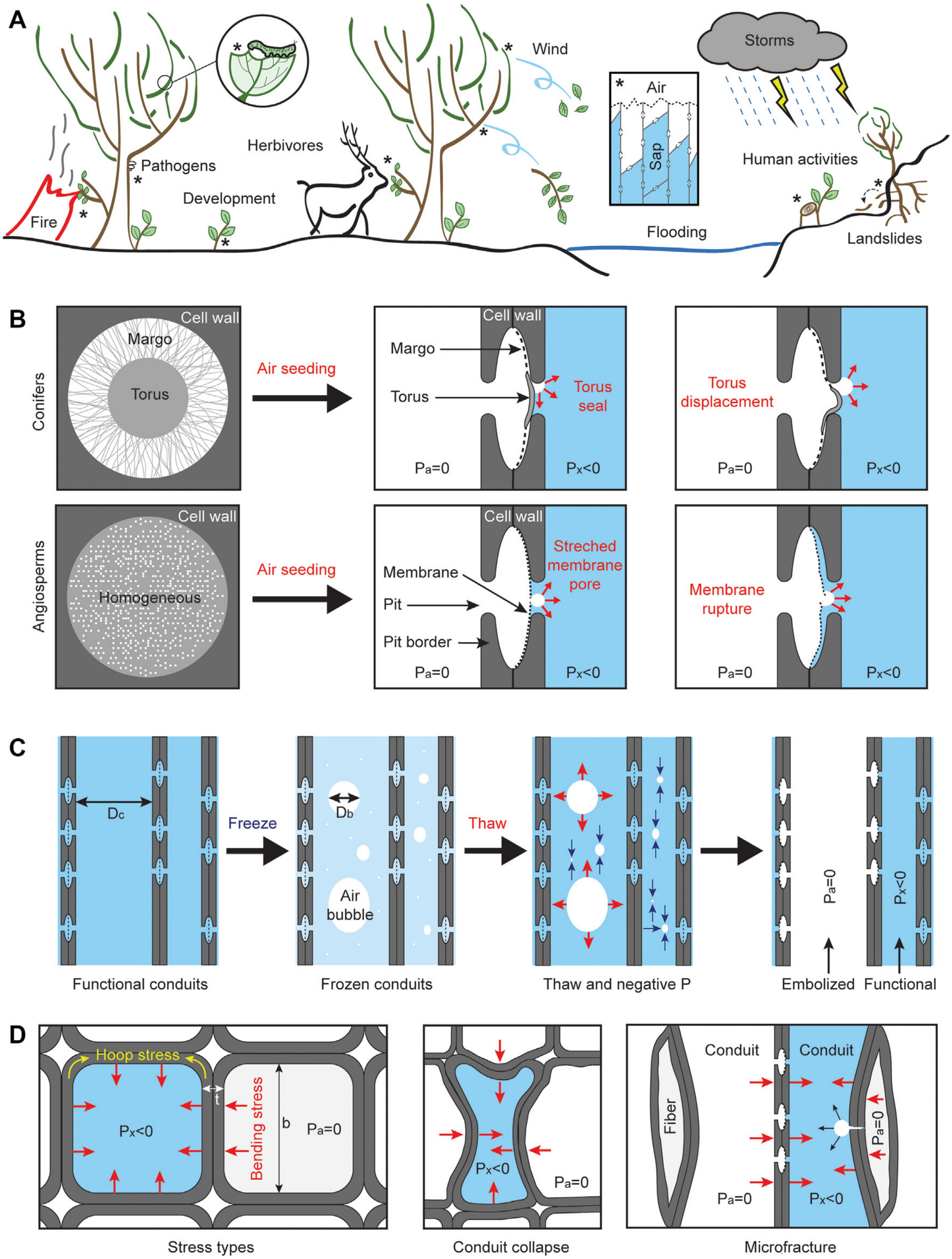

Figure 4. Mechanisms of xylem dysfunction

(A) Mechanical damage and xylem rupture and exposure to air is something that plants face commonly due to storms, wind, herbivores, pathogens, fires, landslides, floods and human activities among many other factors. Inter-conduit pits arrest the leakage of air (insert). **(B)** Air-seeding mechanism under drought stress conditions for conifers and angiosperms. The pressure difference (ΔP) between an air-filled conduit ($P_a = 0$) and a contiguous functional sap filled one ($P_x < 0$) causes the pit membrane to be deflected against the bordered pit wall of the functional conduit. In conifers air is aspirated into the functional conduit when ΔP is greater that the pressure that can be sustained by the torus-bordered pit seal or when ΔP is large enough to displace the torus from its sealing position. In angiosperms air seeding occurs when ΔP is greater than the capillary force of the air-sap meniscus that the largest pore of the pit membrane can sustain or when the membrane ruptures. **(C)** Susceptibility to embolism induced by freeze-thaw cycles depends on the conduit (D_c) and air bubble (D_b) diameters. When the water within a conduit freezes (crystallizes) the air that it contained dissolved in the water comes out of solution forming bubbles. If these bubbles are small enough they can dissolve again (or collapse) when the ice thaws (blue arrows), but if they are large they will expand due to the negative pressure in the conduit until it becomes embolized (red arrows). Conduits with larger diameters are more susceptible to freeze-thaw cavitation. **(D)** Under drought-stress conditions conduits can fail mechanically if they do not support hoop stress (which is thought not to be significant) or bending stress (as shown in transverse section). The amount of bending stress that a conduit can withstand depends on the double wall thickness (t) and the wall span (b). If the pressure is low enough the conduit can collapse or air seeding could potentially occur through microfractures in the wall (as shown in longitudinal section).

of the bubble, the sap surface tension (Γ) and xylem sap pressure (P_x). Cavitation will occur when (Yang and Tyree 1992; Davis et al. 1999):

$$P_X \le P_b - \frac{4\Gamma}{D_b} \qquad (2)$$

where all pressures are relative to atmospheric in Pa, and Γ and D_b are in N m^{-1} and m, respectively. Thus, lower sap pressures and larger bubbles during thawing will induce greater levels of cavitation. Experiments performed on non-transpiring stems support the thaw expansion hypothesis by specifically showing that the embolism arises during the thawing phase, not during the freezing phase (Utsumi et al. 1999; Mayr and Sperry 2010). Low or zero transpiration is likely the natural situation during winter.

Species with larger conduits and under higher water stress levels (lower P_x) have been shown to be more vulnerable to freeze-thaw cavitation (e.g., Sperry and Sullivan 1992; Davis et al. 1999; Mayr et al. 2003b; Pittermann and Sperry 2006; Charrier et al. 2014). Conduit diameter, rather than length, is the important dimension determining susceptibility to freeze-thaw cavitation (Davis et al. 1999; Pittermann and Sperry 2003, 2006). This is thought to result from sap freezing from the conduit walls towards the center, thus larger conduit diameters lead to formation of larger bubbles as gas is pushed out of solution at the ice front as it progresses towards the center, and larger bubbles are more prone to expand during thawing under negative pressure as determined by Eq. 2 (Pittermann and Sperry 2006). Narrower conduits also require lower temperatures for ice nucleation providing additional resistance to freeze thaw cavitation (Lintunen et al. 2013).

Other factors that affect freeze-thaw cavitation are the speed of ice formation and thawing, the number of cycles, and the minimum ice temperature. Theoretical calculations indicate that the larger the conduit diameter or slower the freezing velocity, the greater are the chances for a successful bubble formation to occur via gas segregation (Sevanto et al. 2012). Faster thaws can create more embolism, possibly because they minimize the time for bubble dissolution prior to the renewal of negative liquid pressures (Langan et al. 1997). The number of freeze-thaw cycles may increase the probability of a bubble large enough to trigger cavitation (Mayr et al. 2003a; Mayr and Sperry 2010). Lower freezing temperatures have been reported to produce greater cavitation due to freeze-induced redistribution of water (Ball et al. 2006) and temperature-dependent decreases in ice water potential that affect bubble formation during freezing and air-seeding (Charrier et al. 2014). Some experiments that infer embolism from acoustic emissions suggest that cavitation can also occur during the freezing phase (Mayr and Zublasing 2010; Charrier et al. 2014). Freezing-phase cavitation is certainly a possibility when stems are frozen while the canopy is actively transpiring. Ice blockage could cause downstream liquid pressures to plummet, inducing cavitation either by air-seeding or at the ice-liquid front (Cochard et al. 2000).

Failure by conduit collapse

Xylem conduit walls must be reinforced with lignin and a thick secondary layer to resist collapse by internal negative pressure (Figure 4D; Hacke et al. 2001a). To a first approximation, the strength of the double wall between adjacent conduits is governed by its "thickness-to-span ratio": the thickness of the double-wall (t) divided by the width of the wall (b). To maintain a given strength, wider conduits must grow thicker walls. The thickness-to-span ratio of the wood cells also influences wood density. Species that can develop very negative sap pressures without cavitating tend to have high thickness-to-span ratios and denser wood, presumably to avoid conduit collapse. It is possible, though direct evidence is lacking, that air-seeding could occur through wall microfractures (Figure 4D; Jacobsen et al. 2005). Actual conduit collapse has been observed in lignin-deficient poplar mutants (Kitin et al. 2010) and under natural conditions in pine needle tracheids (Cochard et al. 2004) and transfusion tracheids of *Podocarpus grayi* (Brodribb and Holbrook 2005). In the latter two examples, collapse was reversible.

Other causes of xylem dysfunction

Vascular pathogens can disrupt water transport by conduit degradation and occlusion or by alteration of sap properties. In Dutch elm disease, a vascular wilt disease caused by the fungi *Ophiostoma ulmi* and *O. novo-ulmi* (Brasier 2000), cavitation has been observed prior to vessel blockage (Newbanks et al. 1983). Enzymatic degradation of vessel walls may cause cavitation by providing entry sites for air seeding either through the secondary wall or through weakened pit membranes, as also observed in *Xylella fastidiosa* infected grapevines (Pérez-Donoso et al. 2010). Infection may also reduce sap surface tension leading to air-seeding at less negative pressures. These effects can be enhanced by a reduction in conductivity due to direct vessel blockage by the pathogen and degradation debris, or by tyloses and gels produced by the elm as a defense response (Figure 5A; Urban and Dvořák 2014; Venturas et al. 2014; Li et al. 2016). Vessel and pit morphological and chemical characteristics also affect the speed of *Ophiostoma* spp. colonization (Martín et al. 2007, 2009, 2013). Desiccation due to xylem cavitation also seems to be the ultimate cause of tree death in pine wilt disease, caused by the pinewood nematode, *Bursaphelenchus xylophilus* (Kuroda 1991; Wang et al. 2010). The spread of cavitation caused by pine wilt disease has been confirmed with magnetic resonance imaging among other techniques (Utsuzawa et al. 2005). During pine infection the production and accumulation of volatile terpenoids, which are hydrophobic and have lower surface tension than water, nucleate bubbles that result in cavitation and embolism of tracheids (Kuroda 1991; Wang et al. 2010). The spread of fungi through the xylem that results in reduced sap flow also appears to be the mechanism of tree mortality by pine beetle infestations (Hubbard et al. 2013).

Fire treatments have been shown to cause xylem dysfunction reducing sap flux density (Ducrey et al. 1996) and functional xylem area (Balfour and Midgley 2006). The mechanisms by which fire induces cavitation are actually air-seeding and mechanical failure. Heating caused by fire reduces sap surface tension (Γ) and, consistent with Eq. 1, the pressure at which cavitation by air-seeding occurs (Michaletz et al. 2012). Xylem dysfunction by conduit deformation is enhanced by thermal softening of cell wall polymers (Michaletz et al. 2012; West et al. 2016). In addition, the fire heat plume increases the vapor pressure deficit to which plants are exposed, potentially dropping xylem pressure (via rapid increase in E) and inducing air-seeding (West et al. 2016).

VULNERABILITY CURVES

Xylem vulnerability curves (VCs) quantify an organ's resistance to xylem cavitation. They are at the heart of much of plant hydraulics research; hence we dwell on their technical underpinnings. Their "y" axis shows the amount of embolism induced by the exposure of the xylem to an "x" axis value for xylem pressure

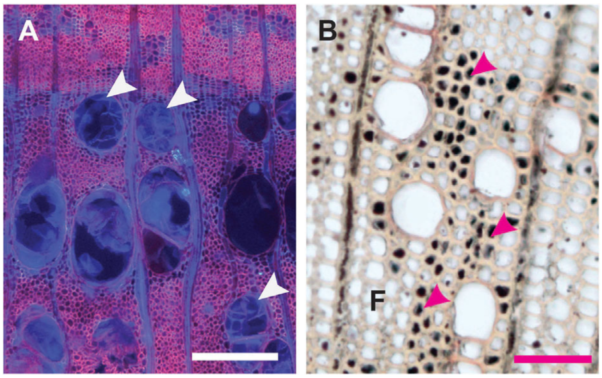

Figure 5. Functions of living cells within the xylem
(A) Field elm (*Ulmus minor*) vessels occluded with tyloses or gels (arrows) produced by contact cells as a response to Dutch elm disease infection. Scale bar 100 μm. Photograph: Juan Antonio Martín. **(B)** Cross-section from a boxelder (*Acer negundo*) branch collected in October after the growing season. Living cells (mainly fibers, F) are packed with starch granules (stained black with lugol solution; arrow heads). Scale bar = 50 μm.

(Figure 6). The VC methodologies differ in how the embolism is induced, and how the embolism is quantified (Table 1). In many cases, multiple combinations are possible, making for a variety of VC types which may suit a corresponding variety of experimental purposes.

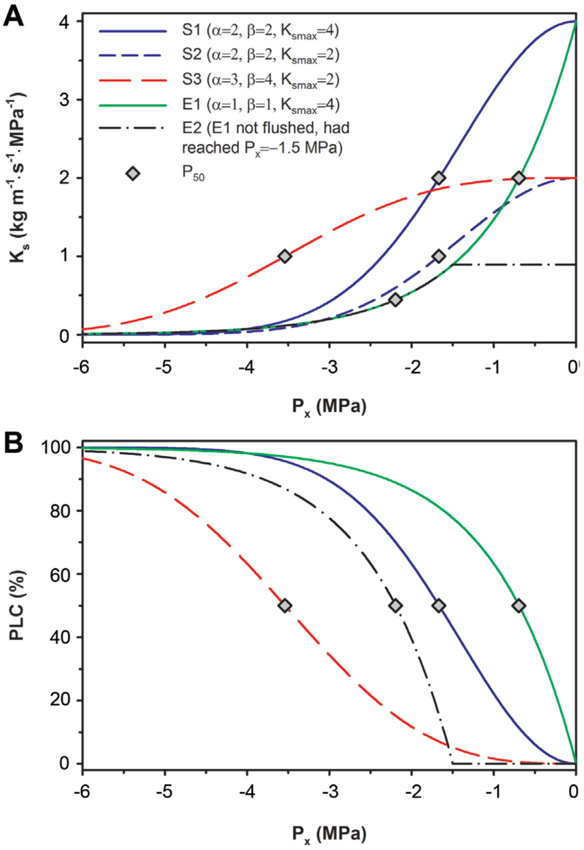

Figure 6. Hydraulic vulnerability curves (VC): shape and the PLC problem

(A) Theoretical VCs represented as losses in K_s vs. xylem sap pressure (P_x). Curves are Weibull functions (Eq. 4; coefficients and K_{smax} as indicated). Pressures at 50% loss of K_{smax} (P_{50}) indicated by symbols. S1–S3 curves are sigmoidal in shape. E1 (green) curve is “exponential” in having an abrupt initial decline in K_s. Dash-dotted E2 curve is the same as E1, except that embolism formed by exposure to $P_x = -1.5$ MPa was not removed (K_{smax} is reduced). Pre-existing embolism changes the curve shape (to sigmoidal) and the P_{50} (from −0.7 to −2.2 MPa). **(B)** The same VCs plotted as PLC vs. P_x reduces information content. Sigmoidal VCs S1 and S2 become identical as PLC, however, S1 could be considered more resistant than S2 because it has a greater K_s at the same P_x. S3 is more resistant than S2 in both K_s and PLC, but its lower initial K_s than E1 is masked by the PLC metric. The flushed E1 curve appears to be completely different from its non-flushed E2 counterpart when plotted as PLC.

Embolism induction techniques

To construct a water-stress VC, cavitation is induced using one of three main methods: air dehydration, air injection, and centrifugation (Table 1). The “air dehydration” technique consists in evaluating cavitation after whole plants (*in situ* or potted) or excised segments (e.g., large branches) are dehydrated to different P_x (Sperry 1986; Tyree et al. 1992). Though sample intensive, this method best mimics actual drought-stress dehydration and is considered a “benchmark” method (Hacke et al. 2015; Martin-StPaul et al. 2014). The “air injection” method uses positive gas pressure to induce xylem embolism when P_x is typically zero. As noted in relation to the air-seeding mechanism, the positive air pressure required to push air through interconduit pit membranes is approximately equal to the negative pressure required to suck air through them (Sperry and Tyree 1988). The pressure can be applied to stems or roots by air injection through a single cut end (Sperry and Tyree 1988) or through the stem or root surface in a double-ended chamber where the organ runs through the axis (Cochard et al. 1992; Salleo et al. 1992; Sperry and Saliendra 1994). In the latter case it is sometimes necessary to incise the stem or root surface (or use cut lateral branches) to insure sufficient air penetration to the xylem. Air injection can also be applied to individual vessels with a micro-capillary connected to a pressure chamber (Melcher et al. 2003). The “centrifugation” technique generates negative xylem pressures in the centre of the sample during rotation as a result of the centrifugal force (Pockman et al. 1995), analogous to Brigg’s experiments with cavitation in glass capillary tubes. There are three main rotor designs for the centrifugation technique. With the standard rotor design (Alder et al. 1997) the sample is extracted from the rotor and embolism detected by measuring the sample hydraulic conductance (see below), whereas with the “Cavitron” (Cochard et al. 2005), or a modification of the standard rotor (Li et al. 2008), the hydraulic conductance is measured during sample centrifugation. “Freeze-thaw cycles” can be applied in combination with air dehydration or centrifugation to induce freeze-thaw cavitation (Sperry and Sullivan 1992; Davis et al. 1999). Air-injection and centrifugation methods have been widely used because

Table 1. Main techniques used for inducing and measuring cavitation. There is a great array of possible combinations between techniques used to induce and measure cavitation (although some are incompatible)

Techniques used to induce cavitation

Stress evaluated	Techniques	Stress applied	Variations
Water stress	Dehydration	Dry down	Native curves (*in situ* plants)
			Air dehydration (potted plants or large excised parts)
	Air injection	Positive gas pressure	Single ended pressure chamber
			Pressure collar or double ended pressure chamber
			Single vessel air injection
	Centrifugation	Rotation ≡ Negative xylem pressure	No flow during rotation (standard rotor)
			With flow measurements performed during rotation
Freezing	Freeze-thaw	Freezing and thawing cycles	Combined with dehydration
			Combined with centrifugation

Techniques used to measure cavitation

Measured variable	Techniques	Description (specific variables)
Conductance	Conductivity apparatus	Flow is measured gravimetrically with a balance while a known pressure head is applied
	Xy'lem	Flow is measured with a thermal mass flow sensor and the pressure head with a pressure transducer
	HPFM	High pressure flow meter
	Evaporative flux	Flow is measured and the pressure drop driving it is generated by transpiration
	Sap flux	Flow through an organ is evaluated with a thermal mass flow sensor
Acoustic emissions	Acoustic emissions	Ultrasonic acoustic emissions due to cavitation are recorded
Images	Active staining	A stain solution is taken up by transpiration or perfused through xylem and functional conduits become stained whereas non-functional ones do not
	Advanced imaging	High resolution X-ray tomography (HRCT), magnetic resonance imaging (MRI) or neutron radiography is used to visualize fluid or air filled conduits
	CryoSEM	Samples are frozen and cryogenic stage surface electron microscopy is used to identify air and ice filled conduits or conduit deformation
Air flow	Air injection	Pressure at which air seeds through the sample is measured
		Air flow through the sample under positive pressure is measured
	Pneumatics	Air flow through the sample under a vacuum is measured

they have several advantages over air dehydration such as requiring less plant material, being less time consuming, and reducing sample variability since several pressures can be evaluated on the same segment.

Embolism measurement techniques

Many techniques have been developed for quantifying the embolism that results from xylem cavitation (Table 1). Most commonly, embolism is measured by its effect on reducing the hydraulic conductance

(k = flow/pressure difference) of pressure-driven water flow through the sample xylem. A hydraulic conductivity apparatus measures the flow rate through a stem or root segment with an electronic balance at a known applied pressure gradient (Sperry et al. 1988). A low pressure difference (usually 1–3 kPa) is used to avoid displacing or dissolving emboli in the sample (e.g., Hacke et al. 2015). Sometimes a higher pressure gradient is used if xylem flow resistance is high and conduits small. If conduits are longer than the sample (and hence open at both ends) the pressure head should be lower than what conduit capillary forces can withstand (Eq. 1). Hydraulic conductance is calculated dividing the flow rate by the applied pressure difference. Ideally, the net flow rate should be measured, or alternatively, k should be calculated from the slope of flow vs. applied pressure. Either approach corrects for a typically non-zero flow intercept (i.e., measurable flow at an applied pressure head of zero; Torres-Ruiz et al. 2012). Hydraulic conductance measurements can also be made on detached shoot (branched stem + leaves) or root systems by measuring the slope of flow rate into the cut base of the system vs. applied vacuum (Kolb et al. 1996) or positive (Yang and Tyree 1994; Tyree et al. 1995) pressure. The “high pressure flow meter” (HPFM) uses positive pressure, which can act to reverse embolism, and over-estimate k in embolized plants.

An alternative to measuring k with experimentally induced pressure-controlled flow is to use leaf transpiration to induce flow (Yang and Tyree 1993). The whole-plant k of intact plants can be estimated by dividing trunk sap flow (Marshall 1958; Granier 1985; Steinberg et al. 1989) by the soil-to-leaf pressure drop measured with the pressure chamber. With the appropriate range of xylem pressures, this method can yield a VC for the whole plant (e.g., Baert et al. 2015). The same approach can be used to measure k on detached leafy shoots or individual leaves, where transpirational uptake into the cut stem or leaf base is directly measured, and the leaf xylem pressure subsequently measured with a pressure chamber (Sack et al. 2002; Sack and Scoffoni 2012). This technique, however, cannot distinguish between changes in k caused by xylem embolism from those due to changes in permeability of the extra-xylary water pathways.

Hydraulic conductance can be standardized for sample length to obtain hydraulic conductivity (K_h = flow rate divided by pressure gradient) and further standardized for cross sectional area to give area-specific hydraulic conductivity (K_s = flow rate per cross-sectional area divided by pressure gradient). The k can also be standardized by leaf area distal to the measured section (leaf specific conductivity, K_L = flow rate per leaf area per pressure difference). Regardless of how hydraulic conductance is standardized for size ($K' = K_h, K_s, K_L$), it is often further normalized relative to its initial, maximum value, prior to experimental embolism induction (K'_{max}). A “percentage loss of hydraulic conductivity“ (PLC) is calculated as:

$$PLC = 100 \cdot \left(1 - \frac{K'}{K'_{max}}\right) \tag{3}$$

Hydraulic conductance data are plotted vs. the corresponding P_x, and usually fitted to functions for comparison and for obtaining commonly used parameters such as the pressure at which 50% of conductivity is lost (P_{50}). VC shapes depend on xylem characteristics and, in theory, can be any shape as long as hydraulic conductance decreases or maintains itself equal while P_x drops (i.e., conductance cannot increase as P_x drops). Common functions used to fit VC data are linear, polynomial, exponential, Weibull, Gompertz, and sigmoid exponential (Pammenter and Van der Willigen 1998). The VCs in Figure 6 were constructed with the following Weibull function:

$$K' = K'_{max} \cdot e^{-\left(\frac{-p_x}{\beta}\right)^{\alpha}} \tag{4}$$

where α and β are, respectively, the scale and shape parameters, and K' is K_h, K_s or K_L. VCs constructed with absolute values of hydraulic capacity (K') compare the plant's actual transport capacity and are often preferable to PLC-based curves. For example, a species with a high K'_{max} which is at 80 PLC can actually have a greater water conducting capacity than another species with low K'_{max} at 5 PLC (Hacke et al. 2015). In either situation, the VC also depends on whether a sample has its native embolism reversed or not prior to curve generation, because this will alter K'_{max}. Embolism reversal is achieved by flushing at moderately high pressures (usually 100–200 kPa) or vacuum infiltrating under filtered measuring solution (e.g., Hacke et al. 2015). Vacuum infiltration is recommended for conifers as flushing may deflect and damage the torus-margo pit membranes (Hietz et al. 2008).

Hydraulic conductivity measurements are usually performed with a 10–30 mM KCl solution to standardize for ionic effects on pit membrane flow resistance (Zwieniecki et al. 2001; Gasco et al. 2006; Nardini et al. 2007). In some cases 1 mM $CaCl_2$ is added because of the additional presence of low levels of Ca^{+2} in sap (Bouche et al. 2016). The added calcium ions can reduce sensitivity to KCl in some, but not all species (Nardini et al. 2007). It is important that the solution is filtered (0.1–0.2 μm filter) to avoid potential reductions in conductivity due to pit membrane clogging (e.g., Hacke et al. 2015). In addition, the solution must not be supersaturated with air to avoid gas bubbles coming out of solution during measurements that may induce conductivity losses. This is especially important if centrifugation methods are used for constructing the VC. Although there is no evidence that xylem sap is degassed *in vivo*, degassing is a useful precaution for avoiding any super-saturation of the measurement solution.

Rather than measuring the hydraulic consequences of embolism, some methods are based on the acoustical detection of the initiating cavitation event. Acoustic emission (AE) monitoring was one of the first methods used to measure cavitation (Milburn 1973; Tyree et al. 1984). With this technique VCs are generally plotted as the percentage of cumulative AEs at each P_x (e.g., Kikuta et al. 1997; Rosner et al. 2006). The AE method is non-invasive, but only provides indirect evidence of xylem embolism since it is not obvious how much loss in k is produced with each AE, plus AEs can be generated in large numbers by processes other than cavitation within xylem conduits (Kikuta et al. 1997).

Imaging embolism is another important way to quantify embolism, and it also provides information on which sapwood areas or conduits are functional. Active xylem staining is performed by allowing a transpiring branch to uptake a dye solution (usually basic fuchsin, acid fuchsin, crystal violet, or safranin) or by perfusing a dye solution at low pressure through the sample (e.g., Newbanks et al. 1983; Sperry 1986; Jacobsen et al. 2007). Functional conduits become stained as dye flows through them. Then sections are prepared and images taken with a light microscope for their analysis. Double staining techniques (i.e., before vs. after embolism reversal) can also be performed to determine if nonfunctional conduits are embolized or permanently blocked, for example, by gels and tyloses (Sauter 1984). The spreading of stain during sample preparation can be a limitation of these methods (Newbanks et al. 1983).

Cryo-scanning electron microscopy (cryoSEM) can be used to determine which vessels are water filled and which embolized (Canny 1997). However, care must be taken to prove that the embolism observed was not caused by the freezing of the sample (Cochard et al. 2000). More sophisticated techniques such as high-resolution magnetic resonance imaging (MRI) (Holbrook et al. 2001), high resolution X-ray tomography (HRCT) (Brodersen et al. 2010, 2011) and neutron radiography (Tötzke et al. 2013) allow visualizing embolized conduits both in intact plants and in excised segments. Of these methods the most widely used is HRCT due to its high resolution (Brodersen et al. 2010, 2011). These methods allow three-dimensional (3D) visualization of the vascular network. However, they are limited in the size and type of samples that can be imaged, the artificial canopy environment, and difficulty of access for making accurate measurements of xylem pressure and other physiological variables. Also, it can be difficult to distinguish actively conducting conduits from immature ones, or those occluded with gels (Pérez-Donoso et al. 2007; Jacobsen and Pratt 2012; Jacobsen et al. 2015). In addition, it is not trivial to predict k of an axis or plant from the spatial distribution of imaged embolized conduits. Although the Hagen-Poiseuille equation can provide estimates of individual lumen conductance (Giordano et al. 1978; Lewis and Boose 1995), the flow resistance of the interconduit pit connections and perforation plates (in vessels) as well as the influence of 3D organization complicates up-scaling to the organ or plant level. A new optical method also allows visualizing the spatial-temporal spread of emboli through leaf vein networks by evaluating rapid changes in light transmission caused by cavitation events (Brodribb et al. 2016).

Another set of techniques are based on air-flow through samples for assessing embolism and constructing VCs. Single vessel air injection (Melcher et al. 2003) registers the gas pressure at which bubbles seed through conduit end-walls, and a VC can be plotted as a the cumulative frequency of conduit air-seeding pressures (Christman et al. 2009, 2012; Venturas et al. 2016b). The fact that pressure-driven air flow increases through an excised sample as a greater proportion of conduits are embolized has been used to estimate VCs from pneumatic conductivity through segments (Ennajeh et al. 2011). A recent method estimates the volume of embolism in dehydrating shoot systems by measuring air flow from the cut end of the shoot induced by a partial vacuum (Pereira et al. 2016).

CURRENT DEBATES

The inherent challenges of working with water in a metastable state have always required methodological vigilance in the plant hydraulics field. It has been learned, for example, that one cannot puncture a xylem conduit with a cell pressure probe and expect to consistently avoid cavitating the metastable liquid phase, particularly at native xylem pressures below −1 MPa (Tyree 1997; Zimmermann et al. 2004). Current debates of methodology and physiological process have been inspired by two seemingly odd, but generally reproducible observations: the apparent active refilling of conduits despite negative xylem pressure, and "exponential" vulnerability curves.

Refilling of embolized conduits

Reductions in *k* due to cavitation and embolism can reduce productivity and pose a threat to plant survival; therefore, understanding how plants repair damage to their transport system is of great importance. Plants with secondary growth can of course grow new water-filled conduits, but a potentially cheaper and shorter-term alternative is refilling embolized conduits (Nardini et al. 2011). Refilling has been documented during specific periods of the year or at night when very high or even positive pressures (above atmospheric, via osmotically generated root pressure) can be generated in the xylem. Under these conditions, xylem pressures rise above the capillary threshold for the conduits (defined in Eq. 1), allowing the embolized conduit to take up water and compress the gas above atmospheric, leading to eventual bubble dissolution (Sperry et al. 1987; Yang and Tyree 1992; Cochard et al. 1994; Hacke and Sauter 1996; Nardini et al. 2011). We refer to this non-controversial type of refilling as "refilling by xylem pressure", meaning that the embolized conduit is being pressurized by the bulk xylem pressure. The exact P_x required, and kinetics of the process, depend on the amount of gas dissolved in the sap, the size of the embolism, and tissue anatomy (Yang and Tyree 1992).

Oddly, not all claims of refilling can be explained in this way. Since at least the 1990s (e.g., Borghetti et al. 1991) there have been reports of refilling despite the bulk xylem sap being *more negative than* the capillary threshold. If true, this is remarkable because it suggests that either Eq. 1 is not always correct, or what is more widely thought, that water is actively pumped into embolized conduits and kept there at pressures above the capillary threshold (and above the surrounding xylem) long enough to refill the conduit. We herein refer to this alternative as "refilling against xylem pressure", because the embolized conduit is being pressurized above the bulk xylem pressure.

Evidence for refilling against xylem pressure has been frustratingly equivocal because of the discovery of a number of measurement artifacts. Some of the earliest reports of refilling against xylem pressure came from experiments where embolism was induced in intact plants by air-injection (Salleo et al. 1996; Tyree et al. 1999). However, it has been suggested (with some evidence) that the appearance of embolism and refilling cycles in these experiments could be created by the supersaturation of xylem water during air injection (Wheeler et al. 2013). Evidence from cryoSEM observations of xylem "flash-frozen" *in situ* (e.g., Canny 1997; McCully 1999) was discounted once it was found that freezing under negative pressure could cause embolism in proportion to the rate of transpiration, creating the illusion of an embolism-refilling cycle (Cochard et al. 2000). Subsequent evidence from diurnal cycles in PLC of excised segments has also been found, in at least a few cases, to result from an "*excision artifact*" (Wheeler et al. 2013). Cavitation is thought to be triggered by the edge of the cutting device or by impurities and microbubbles that flow into the sample during excision (Wheeler et al. 2013). Keeping the water in which samples are cut and prepared clean is important to avoid impurities entering conduits through their cut end. Recent HRCT imaging supports the supposition that embolism is artificially introduced during cutting of a stem whose xylem is under negative pressure, even if this is done under water as is standard (Torres-Ruiz et al. 2015). The more negative the xylem pressure during cutting, the greater the excision artifact, hence diurnal pressure cycles can result in what looks like an embolism and refilling cycle. The excision artifact has led some researchers to go so far as to reject all evidence for refilling against xylem pressure (Cochard and Delzon 2013; Delzon and Cochard 2014).

However, the excision artifact is not as damning as it might seem. Firstly, not all species exhibit the problem (Wheeler et al. 2013; Venturas et al. 2015), and leaves as an organ appear to be immune (Scoffoni and Sack 2015). Secondly, the excision artifact is easily avoided by relaxing the xylem pressures before making the final cut, which can be done by making multiple underwater cuts, gradually clipping the segment down to its final length and removing any superficial embolism or clogging caused by the first cut (Trifilò et al. 2014; Torres-Ruiz et al. 2015; Venturas et al. 2015; Nardini et al. 2017). This precaution was originally recommended by Dixon (1914), and has been widely employed since that time (e.g., Zimmermann 1978; Venturas et al. 2015). In some species, such as *Laurus nobilis*, the opposite problem of passive embolism refilling can result if stems are relaxed too long in water prior to final sample excision (Trifilò et al. 2014; Venturas et al. 2015). However, negligible post-excision refilling was observed in *Vitis coignetiae* based on a recent MRI study (Ogasa et al. 2016). Furthermore, a recent study performed with HRCT in *Laurus nobilis* also showed no increases in PLC following the proper excision protocol (i.e., multiple under-water cuts) and found a good agreement between hydraulic and imaging techniques (Nardini et al. 2017).

In summary, an excision artifact can be avoided by: (i) making multiple under-water cuts of samples originally under tension such that the original cut is at least 1 cm (if not one maximum conduit length) from the final segment end; and (ii) minimizing relaxation time in water (Trifilò et al. 2014; Beikircher and Mayr 2015; Venturas et al. 2015; Ogasa et al. 2016). Both of these practices have been widely used, and it is not obvious that all evidence for refilling against xylem pressure can be dismissed by the excision artifact. This is particularly true since many of these studies show inhibition of refilling by the interruption of phloem transport by girdling or by using metabolic blockers (e.g., orthovanadate), a result which cannot easily be attributed to the excision artifact (e.g., Salleo et al. 1996, 2004; Christman et al. 2012; Trifilò et al. 2014).

In vivo imaging techniques have been able to catch embolism refilling in action (Brodersen et al. 2010; Brodersen and McElrone 2013), but whether this is truly refilling "against" xylem pressure requires better resolution of P_x adjacent to the refilling conduit. In studies on *Vitis*, water can be seen exuding into embolized vessels from adjacent living cells (Brodersen et al. 2010; Knipfer et al. 2016). This is consistent with a Münch-type flow redirected from the phloem towards embolized conduits via ray tissue and xylem parenchyma (Salleo et al. 2004, 2006, 2009; Nardini et al. 2011; Lucas et al. 2013). Exudation may be driven osmotically by accumulation of sucrose or other osmoticum in residual water of embolized conduits (Secchi and Zwieniecki 2010, 2011; Nardini et al. 2011; Ryu et al. 2016), or by pressure-driven flow analogous to water exiting phloem sink cells. Whether the conduit ultimately fills appears to require that the collective rate of exudation into the conduit exceeds drainage from the conduit into the surrounding xylem (Brodersen et al. 2010; Knipfer et al. 2016). The observation of drainage suggests that refilling conduits are not hydraulically isolated by air-blocked pit membrane chambers, as has been speculated (Holbrook and Zwieniecki 1999; Zwieniecki and Holbrook 2000; Vesala et al. 2003). The more negative the P_x, the more likely drainage would exceed exudation, which may limit the refilling to P_x very near the capillary threshold. Given that water drained from refilling vessels would tend to elevate local P_x, it is crucial to measure the local P_x to prove whether the imaged refilling is indeed against xylem pressure.

Exponential vulnerability curves

A second current methodological controversy concerns the accuracy of VCs when performed on long-vesseled material using centrifuge methods (Cochard et al. 2013; Delzon and Cochard 2014; Martin-StPaul et al. 2014). Long-vesseled samples include stems of ring-porous trees, lianas, and roots of many angiosperms. Such VCs typically show an "exponential" shape, wherein hydraulic conductivity drops quickly and significantly as soon as P_x becomes negative, before stabilizing to a long "tail" at more negative P_x (curve E1 in Figure 6). The exponential shape seems odd, because it indicates that many vessels are so vulnerable as to be embolized under typical midday xylem pressures. Careful experiments with the *Cavitron* rotor design (Cochard et al. 2005) have shown that an exponential shape is caused by artifactual embolism of vessels that are long enough to extend from the cut end of the sample to its middle or beyond (Cochard et al. 2005, 2010; Martin-StPaul et al. 2014; Wang et al. 2014; Pivovaroff et al. 2016). In the *Cavitron* procedure, there is water flow through the sample during spinning, and it has been suggested that the artificial vulnerability is due to micro-bubbles or other impurities triggering cavitation as they flow through long vessels towards the centre of the sample where the pressure is most negative (Sperry et al. 2012; Rockwell et al. 2014; Wang et al. 2014; Pivovaroff et al. 2016). In species with short vessels, such impurities are intercepted by pit membranes before reaching the middle of the sample. In light of these results, it has been suggested that *all* exponential VCs are incorrect regardless the method used to obtain them, and that *all* centrifuge methods are prone to an "open vessel artifact" as the phenomenon has been termed (Cochard et al. 2013; Cochard and Delzon 2013).

When all the evidence is considered, however, it is premature to dismiss the validity of an exponential curve shape in every circumstance. The *Cavitron* rotor design may be especially prone to the open vessel artifact, because when the standard rotor design and procedure is used (Alder et al. 1997), extensive testing shows no clear evidence of the artifact (Christman et al. 2012; Jacobsen and Pratt 2012; Sperry et al. 2012; Tobin et al. 2013; Hacke et al. 2015; Pratt et al. 2015). Unlike the *Cavitron*, in the standard rotor there is no flow through the sample during spinning, and there is no need to deliver solution to the sample during spinning, a turbulent process that could create de-stabilizing microbubbles. Both features of the standard rotor may minimize the open vessel issue. But more convincing is that exponential VCs from long-vesseled species can be obtained by methods other than centrifugation. VCs generated using single-vessel air injection or stem-end air injection, and the benchmark method of air dehydration (which is assumed to be the least artifact-prone; Martin-StPaul et al. 2014) can all give exponential VCs (e.g., Christman et al. 2012; Sperry et al. 2012; Yang et al. 2012; Tobin et al. 2013; Hacke et al. 2015; Venturas et al. 2016b). Exponential VCs are also found in root xylem of many conifers (Pittermann et al. 2006a). Although root tracheids are larger than stem tracheids, they are still unicellular and obviously too short to suffer from an open "vessel" artifact.

Exponential curves are also not necessarily as odd as they might appear at first glance. Given the dogma that large conduits are more vulnerable than small ones (see below), it should not be surprising that VCs from material with very large conduits should indicate cavitation at more modest P_x than material with smaller conduits. Large conduits also have a much greater hydraulic conductance than small ones, so exponential VCs typically start at a much higher K'_{max} than a sigmoidal VC. Thus, even after a substantial loss of K' (i.e., a large PLC), the tail end of the exponential VC can exhibit an *absolute* K' that is comparable to the K'_{max} of a sigmoidal curve. This tail can extend to a P_x as negative (or more so) as the end of a sigmoidal curve. Exponential root VCs (e.g., Torres-Ruiz et al. 2012; Pratt et al. 2015) are consistent with their larger conduits, and the fact these upstream organs are exposed to less negative P_x than stems (Figure 2). In some species like *Populus tremuloides* (Venturas MD, Love DM, Sperry JS, 2016, unpublished data) the root curves are exponential but at 90 PLC still have greater K_s than fully hydrated stems ($PLC = 0$) that have sigmoid curves. Exponential curves do not necessarily imply daily cycles of cavitation and refilling as concluded by some researchers (e.g., Cochard and Delzon 2013). While this may occur with some species under specific environmental conditions (e.g., Yang et al. 2012), in other cases the highly vulnerable conduits may become more permanently embolized.

Factors other than conduit size can also influence VC shape, complicating the debate. The same material can have both an exponential and a sigmoidal curve depending on whether embolism was initially reversed (by flushing or vacuum infiltration). An exponential VC can only be measured on refilled material; non-refilled samples will *always* have a sigmoidal VC (as shown in Figure 6) because any vulnerable conduits will already be embolized (Sperry et al. 2012; Hacke et al. 2015). The method to select depends on the question and experimental circumstances; but the difference complicates meta-analyses that attempt to compare VC's across species (e.g., Choat et al. 2012). Short-vesseled species with a sigmoidal VC can also transition to an exponential VC after going through a cavitation and refilling cycle, exemplifying the "cavitation fatigue" phenomenon (Hacke et al. 2001b). Cavitation fatigue has been attributed to the weakening of pit membranes after air-seeding (Hacke et al. 2001b; Hillabrand et al. 2016). Cavitation fatigue appears to be reversible in sunflower, depending on the composition of the xylem sap (Stiller and Sperry 2002). In balsam poplar and trembling aspen, by contrast, pit membranes become irreversibly damaged as a result of drought-induced cavitation (Hillabrand et al. 2016). VCs plotted in PLC terms can also alter their shape solely due to changes in K'_{max} as a result of permanent blockage of conduits with gels or tyloses after samples have been stressed (Jacobsen and Pratt 2012).

SAFETY VS. EFFICIENCY TRADE-OFFS IN XYLEM

Water stress VCs have been measured for many hundreds of species, and show considerable variation. The P_{50} (P_x at 50 PLC) ranges from above −1 MPa to below −10 MPa (Choat et al. 2012). This variation is highly correlated with ecology such that species are generally no more resistant to cavitation than required to maintain transport over the P_x range encountered during their growing season. It is obvious that drier soil in the active rooting zone means more negative P_x, which requires more cavitation-proof xylem for transport maintenance. But it is less obvious why species with a very cavitation-proof xylem tend to be excluded from wet habitats. A general hypothesis is that traits that confer safety from cavitation under low P_x conditions compromise competitive ability under high P_x conditions.

A specific version of this hypothesis is a "safety vs. efficiency" tradeoff wherein traits that provide safety from cavitation also decrease the hydraulic conductance of the xylem, which reduces growth rates under favorable conditions (Hacke and Sperry 2001; Gleason et al. 2015; Pratt and Jacobsen 2017). In support of this hypothesis there is a tendency for negative P_{50} to be associated with reduced K'_{max}, although the trend can be quite weak (Gleason et al. 2015). The weakness emerges from the fact that cavitation resistance and K'_{max} are determined by different combinations of xylem traits. According to the air-seeding mechanism, cavitation resistance increases with lower permeability of the collective inter-conduit pitting (the conduit "end-wall") to air penetration. The safety vs. efficiency trade-off suggests that an air-tight end-wall would necessarily also have a low hydraulic conductance, thus acting to reduce K'_{max}. Curiously, at the individual pit level, there is no evidence for this trade-off. Interspecific comparisons indicate that more air-tight pits do not exhibit lower estimated hydraulic conductance (Wheeler et al. 2005; Hacke et al. 2006). Direct measurements of these crucial pit properties are difficult to achieve (e.g., Choat et al. 2006), but are needed to confirm the lack of a pit-level trade-off. Although there may be no trade-off for individual pits, one could still emerge when the entire end-wall (which can include tens of thousands of pits) is considered. According to the "rare-pit" hypothesis (Wheeler et al. 2005; Hacke et al. 2006; Christman et al. 2009; Lens et al. 2010), end-wall air-seeding pressure results from the single leakiest pit in the vast array of end-wall pits. By chance, the more pits per end-wall, the leakier the end-wall, and the more vulnerable the xylem to cavitation. By the same token, the more pits per end-wall, the greater the end-wall hydraulic conductance, and the larger will be the entire conduit lumen and its hydraulic conductance. The K'_{max} will increase accordingly, because it depends on the series conductance of end-wall and lumen.

The rare pit hypothesis is consistent with a weak P_{50} vs. K'_{max} relationship. The number of end-wall pits per conduit size (lumen length and diameter) is quite variable (Sperry et al. 2005; Wheeler et al. 2005; Hacke et al. 2006). Hence, P_{50} (which depends on pit number) can be partially uncoupled from K'_{max} (which depends in part on conduit size). Safety of large and efficient vessels can also be preserved by not connecting them directly via one end-wall, but connecting them with short "bridges" of small vessels or tracheids (e.g., Carlquist 1985; Brodersen et al. 2013; Cai et al. 2014) whose multiple end-walls greatly reduce the chance of air propagating between the big vessels. There is also evidence of variation in the relationship between end-wall pit quantity and end-wall air-seeding pressure (Christman et al. 2009, 2012; Christman and Sperry 2010; Lens et al. 2010). Pit qualities, such as membrane thickness and chemistry, membrane diameter, pit chamber depth, and aperture size, likely alter the probabilistic link between pit number and collective air-seeding pressure (Christman et al. 2009). Furthermore, K'_{max} can be increased independently of P_{50} simply by adding more conduits per xylem area without changing any other structural feature (Pittermann et al. 2005; Hacke et al. 2006). Finally, modeling studies have shown that the impact of an embolized conduit on total conductance depends on how it is connected to the 3D conduit network (Loepfe et al. 2007).

A broader interpretation of the safety vs. efficiency trade-off includes mechanical safety in addition to safety from air-seeding. As discussed above, conduits that are resistant to air-seeding must also be stronger with a greater thickness-to-span ratio, and hence contribute to denser, more expensive, wood (Hacke et al. 2001a; Jacobsen et al. 2005). A developmental upper limit to wall thickness ultimately limits conduit diameter for a given strength and hence K'_{max}. Thus, large conduits may not be able to support low negative pressures for strength reasons alone, regardless of air-seeding considerations. This strength vs. efficiency trade-off may be the main reason for the P_{50} vs. K'_{max} relationship observed in conifers (Pittermann et al. 2006b). Conifer wood is 95% tracheids by volume, meaning conduit strength and wood strength are highly coupled. Angiosperm wood is generally less than 20% vessels, so its conduit properties can vary more independently from wood-level features. The remaining 80% is largely taken up by fibers (which greatly influence density, strength, and storage) and xylem parenchyma (storage and xylem refilling; Figure 5B).

The safety vs. efficiency trade-off is much more straightforward with respect to freeze-thaw-induced embolism. As noted previously, vulnerability to freeze-induced embolism increases strongly with conduit diameter, consistent with theoretical expectation (see above). The Hagen-Poiseuille equation predicts that hydraulic conductivity of conduit lumens increases with the fourth power of their diameter (Giordano et al. 1978; Lewis and Boose 1995). Hence, resistance to freezing-induced embolism necessarily comes at the expense of conduit-level conducting efficiency. This trade-off is consistent with a general trend towards narrower xylem conduits with increasing freezing threat in diffuse-porous trees (McCulloh et al. 2010; Hacke et al. 2017).

The contrast between conifers and angiosperms exemplifies the complexity of xylem tradeoffs. At first glance, tracheid-based conifer xylem might seem to be hydraulically inferior to vessel-based angiosperms, given that tracheids are roughly 10 times shorter than vessels of the same diameter, and that tracheids do not reach as wide a maximum diameter as vessels (Pittermann et al. 2005). Yet conifers often dominate forests of temperate climates, and whole stem K'_{max} overlaps substantially between diffuse-porous temperate angiosperms and co-occurring conifers (Pittermann and Sperry 2003; Pittermann et al. 2006a,2006b). One reason for this overlap is that diffuse-porous vessels are limited in their diameter to minimize freezing-induced embolism in winter (Hacke et al. 2017). A second reason is that conifers compensate for their "inefficient" tracheids by maximizing their number per wood area, and maintaining several years of functional sapwood (e.g., vs. just a single ring in ring-porous angiosperms). A third, and most interesting reason, is that the torus-margo pit structure of conifer tracheids is approximately 60 times more efficient (per pit area) in conducting water than the inter-vessel angiosperm pit (Pittermann et al. 2005), a feature which compensates for the fact that water must pass these pits roughly 10 times more frequently as it travels up the tree. And notably, this 60-fold increase in pit efficiency has been achieved without compromising safety from air-seeding, because conifers as a group are no more vulnerable to cavitation than angiosperms (Pittermann et al. 2005). Indeed, they tend to maintain larger cavitation safety margins (Choat et al. 2012).

It seems clear that multiple strategies have evolved to balance multiple trade-offs in xylem structure and function, such that ecological parity is approached despite considerable anatomical diversity.

MOLECULAR BIOLOGY OF XYLEM FUNCTION

Genetics of cavitation resistance

Genetic and genomic tools have been used to study drought resistance mechanisms in crops and guide breeding programs (Tuberosa and Salvi 2006; Fleury et al. 2010), and to a lesser extent also in some tree species (Aranda et al. 2012). Few of these molecular studies have focused on xylem cavitation, probably because of the time consuming phenotyping involved (but see Plavcova et al. (2013) for an example where it was performed). Some have evaluated the effect of ploidy levels on hydraulic traits including cavitation resistance (Maherali et al. 2009; Hao et al. 2013), others aquaporins expression and their effect on conductance or refilling (e.g., Hacke et al. 2010; Secchi and Zwieniecki 2010), and several the relationships between population genetic diversity, cavitation resistance and the plasticity of this trait (Aspinwall et al. 2011; Corcuera et al. 2011; Lamy et al. 2011, 2014; Schreiber et al. 2011, 2016; Wortemann et al. 2011; López et al. 2013, 2016). Most of the latter studies found limited genetic effect on hydraulic trait variations which were largely due to phenotypic plasticity, but in *Pinus canariensis* and *Artemisia tridentata* support for local adaptation of traits related to hydraulic safety and survival was also found (Kolb and Sperry 1999a, 1999b; López et al. 2013, 2016). In hybrid poplar clones, genetic variation in cavitation resistance was correlated with average leaf size. Clones with small leaves had more resistant xylem than genotypes with larger leaves (Schreiber et al. 2016); and this finding deserves follow-up experiments.

Many developmental studies have analyzed the genes involved in xylem growth, cell wall deposition and tracheary element maturation (Oda and Fukuda 2014; Ménard and Pesquet 2015; Růžička et al. 2015; De Rybel et al. 2016). Although these latter studies did not evaluate resistance to cavitation, this kind of research could provide promising insights to the plant hydraulics field due to the importance of cell wall and pit membrane development and physical-chemical characteristics in cavitation resistance. Studies focused on secondary cell wall lignification also help understand resistance to conduit collapse (Kitin et al. 2010).

Given the importance of hydraulic traits in plant ecology and performance, there is a huge opportunity for contributions from molecular biology. In particular, it would be a major advance to discover the genetic architecture underlying the VC phenotype. This would open the door to more explicit testing of structure-function physiology (via targeted modulation of gene expression) than would ever be possible using standard physiological experiments.

Aquaporins and plant hydraulics

Flow through the plasma membrane and most inner cell membranes is facilitated by membrane proteins called aquaporins. Depending on cellular localization and sequence homology, aquaporins are divided into subgroups. The most commonly studied subgroup is the plasma membrane intrinsic proteins (PIPs). The functions of PIPs in roots and leaves have been discussed in a recent review (Chaumont and Tyerman 2014). Here we focus on the physiological roles of PIPs located in or near vascular tissue. PIP water channels are prominent features of both xylem and phloem (Hacke and Laur 2016). This suggests that PIPs play important roles associated with long-distance transport (Figure 7).

What functions do aquaporins have in the xylem? Long-distance transport occurs in tracheids and vessels, so why are water channels needed? To answer this question, it is useful to consider that vessels have extensive pit connections with xylem parenchyma cells, and that water is constantly re-distributed between the apoplast (xylem conduits) and symplast (living vascular cells).

The parenchyma cells that specialize in this exchange are called contact cells. These contact cells are sites of increased enzyme activity (Sauter et al. 1973). Contact cells have large vessel-facing pits (Murakami et al. 1999; Plavcová and Hacke 2011) and express high numbers of PIP mRNA (Almeida-Rodriguez and Hacke 2012). These features are consistent with the hypothesis that PIPs are located in the plasma membrane of contact cells to facilitate water exchange between the vessel and parenchyma networks. The direction of water movement will depend on the water potential gradient. The refilling of embolized vessels is one example for the significance of this interface. In this case, water will flow from rays to embolized vessels. To the extent that living parenchyma cells contribute water to the transpiration stream (capacitance; see Pfautsch et al. 2015a), water will flow from rays to water-filled vessels. When transpirational demand is minimal, the direction of flow may change and ray cells may recharge by taking up water from the vessel network.

Aquaporin-mediated water exchange via contact cells also allows for radial water movement from functional vessels to the cambium. This will likely support cambial activity and the expansion of developing vessel elements. The rapid expansion of developing vessel elements is driven by gradients in solute concentration and subsequent water uptake. It is therefore not surprising that PIPs are localized to the plasma membrane of expanding vessel elements (Stanfield et al. 2017). Finally, water is exchanged between xylem and phloem (Münch 1927; Pfautsch et al. 2015b). The exchange of water between the two vascular tissues likely contributes to the establishment of pressure gradients in the phloem.

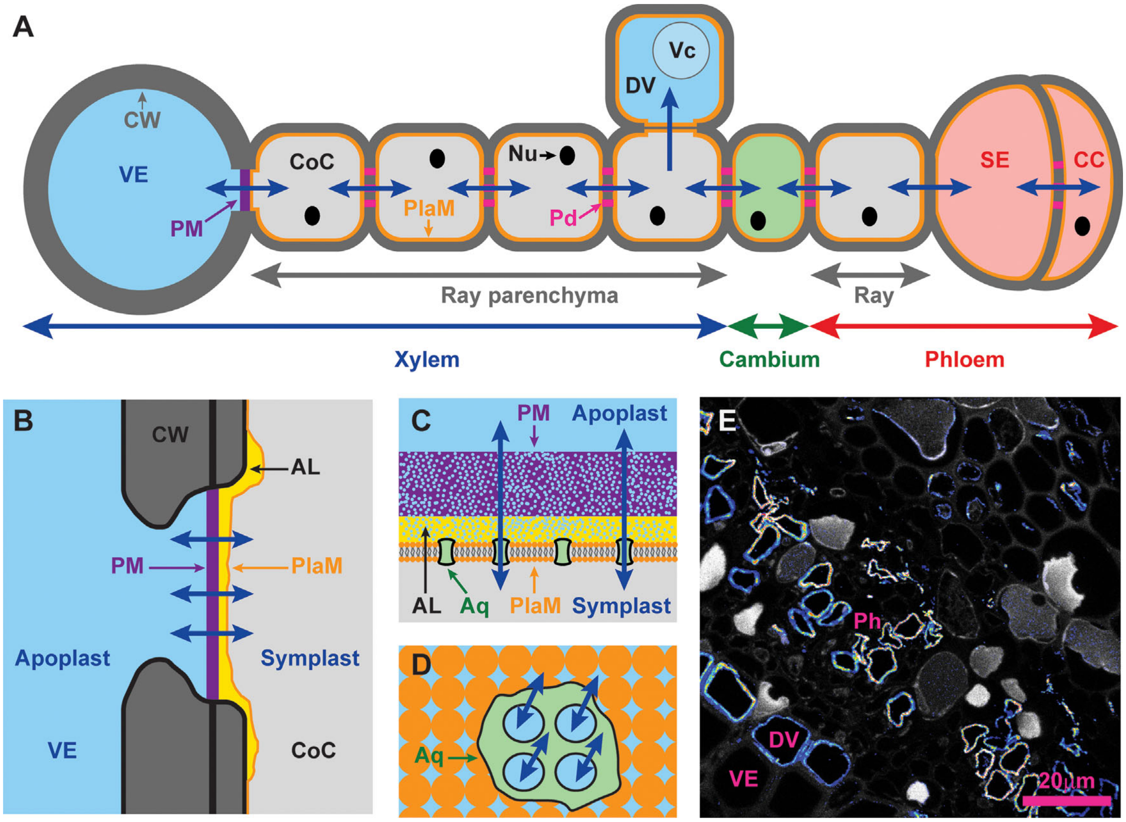

Figure 7. Role of aquaporins in radial water flow
(A) Simplified diagram showing water flow (blue arrows) when water is exchanged between vessel elements (VE), contact cells (CoC), ray parenchyma, sieve elements (SE), and companion cells (CC). It is to be noted that mature VE are dead cells and therefore do not have a plasma membrane (PlaM), nucleus (Nu) nor any other organelles such as vacuoles (Vc). Water exchange between living cells if facilitated by plasmodesmata (Pd). Developing vessel elements (DV) do have a PlaM and water mainly flows into them to facilitate their expansion. **(B)** Detail of a pit connection between a VE and a CoC. Water flows through the pit membrane (PM), an amorphous layer (AL) and the PlaM. Cell wall (CW) is thicker in the VE as it has to support lower pressures. **(C)** Details showing how aquaporins (Aq) facilitate water flow through the PlaM at a pit connection. **(D)** Aquaporins form tetramers with four individual channels through which water molecules can flow in single file configuration. **(E)** Confocal laser scanning micrograph showing the localization of PIP2 (water channel) proteins in a balsam poplar (*Populus balsamifera*) leaf midvein. The image is color-coded: black and grey show background; yellow/white shows strong signal intensity. Strong PIP2 signals were found in two cell types, the plasma membrane of phloem sieve tubes (Ph) and in the plasma membrane of developing vessel elements (DV). Micrograph: Ryan Stanfield. Scale bar = 20μm.

The picture emerging from these considerations is that radial water exchange (and water moving between the symplast and apoplast) is potentially important, yet it remains understudied and difficult to quantify. A more holistic view of xylem transport will include radial water exchange in addition to long-distance axial flow. The same statement can be made for phloem transport (van Bel 2003; Lucas et al. 2013), but this is beyond the scope of this review.

Aquaporin activity will also influence the hydraulic conductance of the "*extra-xylary*" flow path of the transpiration stream in the roots and leaf tissue. If the extra-xylary conductance declines faster with P_x than the xylem component, it can significantly reduce whole-plant hydraulic conductance independently of the xylem VC. Recent work on whole leaf vulnerability curves (including the extra-xylary component) reports an often extraordinarily sensitive decline in leaf hydraulic conductance with P_x, with virtually all of the decline attributed to extra-xylary tissues (Scoffoni et al. 2017). Any role of aquaporins is unknown. These results deserve further confirmation, however, because the reported declines in detached leaf k are quite severe (Scoffoni et al. 2017), even going to zero at values of P_x where intact plants of the species are still actively transpiring and have significant whole plant hydraulic conductance (e.g., *Malosma laurina*; Taylor-Laine et al. 2016). At the root end of the flow path, declines in extra-xylary conductance (together with xylem cavitation) are important in disconnecting absorbing roots from drying soil. This disconnection acts to moderate the P_x of the active rooting zone in deeper-rooted plants, and in shallow rooted CAM plants it acts to keep stored water from being sucked back out of the plant by drying soil (North and Nobel 1997, 1998).

MODELING PLANT RESPONSES TO ENVIRONMENT AND DROUGHT MORTALITY

Extensive tree and shrub diebacks and die-offs due to drought stress have been reported globally (Figure 8; e.g., Breshears et al. 2005; Allen et al. 2010; Anderegg et al. 2012). The physiological processes and mechanisms underlying drought mortality are far from being fully understood, in part due to complicated interactions with other factors such as pests and diseases, and the difficulty to determine precisely when a plant is dead (Sala et al. 2010; McDowell et al. 2013; Sevanto et al. 2013). Three main drought-mortality mechanisms, that can occur simultaneously, have been proposed: (i) hydraulic failure of the vascular system, (ii) carbon starvation, and (iii) pest or disease attacks due to the reduced vigor of stressed plants (McDowell et al. 2013). However, hydraulic failure or damage to the vascular system seems to be the most consistent and common element associated with drought mortality (Kukowski et al. 2013; Anderegg et al. 2015b; Rowland et al. 2015; Anderegg et al. 2016; Rodríguez-Calcerrada et al. 2017).

Hydraulic traits are consequently well correlated to species drought mortality (e.g., Pratt et al. 2014; Anderegg et al. 2016; Venturas et al. 2016a). Several studies show that species with very resistant xylem are not always the ones with greater survival under severe drought conditions (e.g., Piñol and Sala 2000; Rice et al. 2004; Venturas et al. 2016a). This is consistent with all species maintaining an approximately similar margin of safety from hydraulic failure regardless of habitat, in part through stomatal control of transpiration and P_x (Choat et al. 2012). Furthermore, a climatic drought can induce very different P_x values across species of the same locality chiefly because of differences in where the active rooting zone is located in relation to the hydrologically-mediated soil moisture profile. Therefore, in order to predict species vulnerability to drought we need to know at a minimum its VC, root distribution, and its stomatal response to environmental cues (which determines E and P_x).

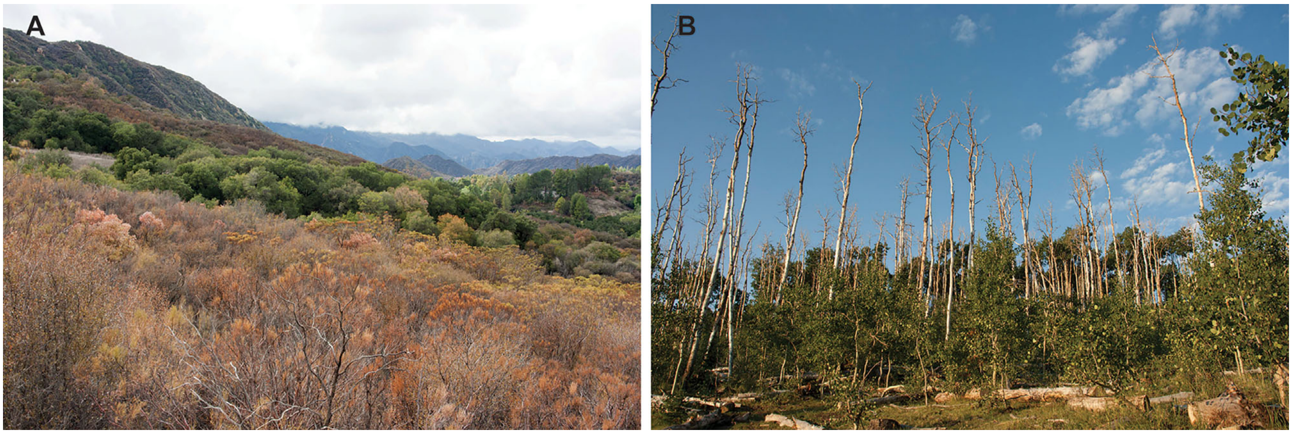

Figure 8. Drought induced dieback and mortality
(A) Diverse chaparral shrub community showing extensive dieback and mortality in California during the 2014 historic drought. **(B)** An aspen stand recovering after die-off presumably triggered by drought stress in Southern Utah.

Modeling stomatal behavior is most challenging, because stomatal aperture responds to diverse environmental cues: soil moisture, atmospheric vapor-pressure deficit, light, and CO_2 concentration. Mechanistic models of stomatal regulation are very complex and far from complete (Li et al. 2006; Buckley and Mott 2013). Consequently, most ecosystem- or land-surface models employ empirical models which need to be calibrated for species and circumstance. Such models are necessarily of limited predictive value, and tend to perform poorly under drought conditions (Powell et al. 2013). An alternative is to assume stomatal regulation optimizes the trade-off between photosynthetic opportunity (which can be modeled from biochemical capacity; Farquhar et al. 1980), and the cost of the associated transpiration. Initial progress was hampered by the lack of a quantitative model for the cost of transpiration (Cowan and Farquhar 1977; Buckley et al. 2017). The subsequent discovery of plant VCs and attendant hydraulic theory have enabled the cost of transpiration to be quantified as the risk of hydraulic failure from cavitation and rhizosphere drying (Tyree and Sperry 1988; Jones and Sutherland 1991; Sperry et al. 1998). A new optimization model uses soil-to-leaf (whole plant) vulnerability curves to calculate the "*water supply function*" (E vs. P_x relationship) for each modeling time step. This function determines how the proximity to hydraulic failure decreases as stomata open and E rises (Sperry and Love 2015; Sperry et al. 2016). The supply function, in combination with leaf energy balance and biochemical models of photosynthesis, is used to calculate the corresponding "instantaneous carbon gain" function (assimilation rate, A vs. P_x) for the same time step. The optimal stomatal conductance (and E, P_x, A, etc.) for that time step is where the relative gain minus the relative hydraulic risk (the instantaneous profit) is maximized (Figure 9; Sperry et al. 2017; Wolf et al. 2016). This relatively simple optimization model produces the expected (and observed) stomatal response trends under a great variety of environmental conditions (combinations of light, CO_2, soil dryness, atmospheric dryness) without the need of knowing the mechanisms underlying stomatal control (Sperry et al. 2017). This approach demonstrates that plant hydraulics can provide the "missing link" between environmental

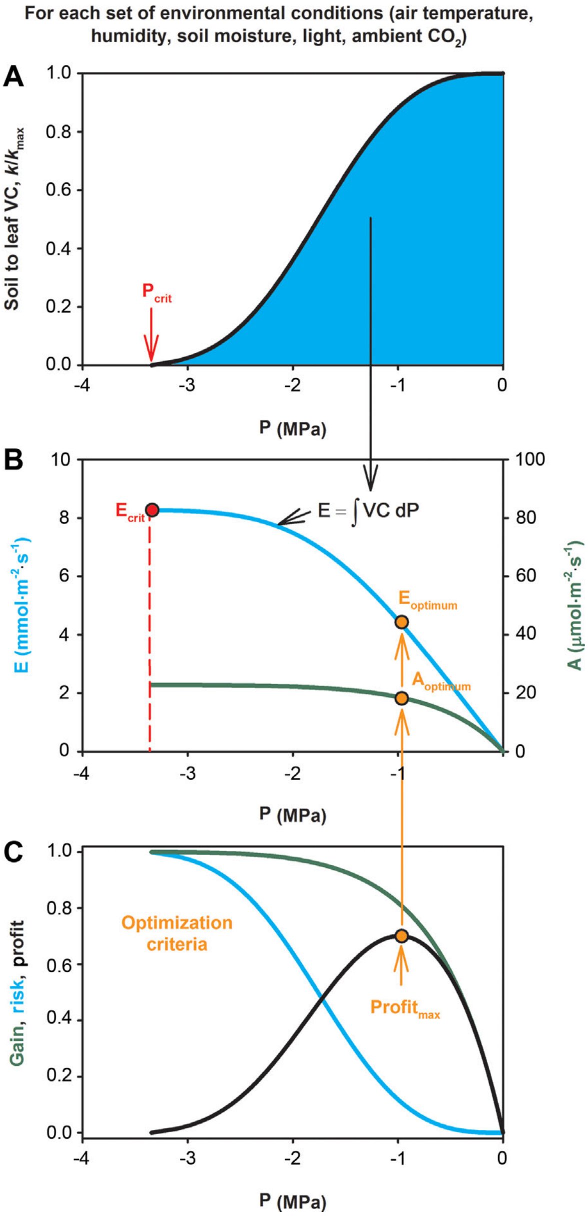

Figure 9. Conceptual framework for stomatal optimization of hydraulic and biochemical limitations

For each modeling time step (and set of environmental cues) a water supply function (E vs. P_x, blue curve in panel B) can be calculated by integrating the whole plant vulnerability curve (panel A). The supply function is a curve of increasing hydraulic risk as E and P_x approach their hydraulic limit at zero hydraulic conductance (E_{crit}, P_{crit}). This transpiration supply function is associated with a corresponding carbon assimilation function (A vs. P_x, green curve, panel B), which can be computed from the supply function and biochemical capacity for photosynthesis. The optimum stomatal conductance at a given instance (at optimization symbols) is located where the relative carbon gain minus the relative hydraulic risk (the profit) is maximized (panel C; for more details refer to Sperry et al. 2017).

cues and stomatal responses for improving the predictions of land-surface models, particularly under drought conditions (e.g., Mackay et al. 2015; Tai et al. 2017). At the same time, the model predicts the degree of hydraulic failure and hence risk of mortality.

In view of the potential for plant hydraulics to improve our understanding of drought responses, there is an even greater need to understand and characterize the VCs of plant organs. Currently, there is much more information available on VCs of small stems than of roots, leaves or main stems, yet we know that plants can be hydraulically "segmented" with roots and leaves often being more vulnerable to cavitation and conductance loss than stems (Tyree et al. 1993; Tsuda and Tyree 1997; Pivovaroff et al. 2014; Wolfe et al. 2016). We also require better understanding of plasticity and regional and seasonal changes in VCs (Jacobsen et al. 2014; Anderegg 2015) as well as VCs' changes due to interactions with other factors such as fire, pathogens, life stage, and regeneration dynamics (Jacobsen et al. 2016; Martínez-Vilalta and Lloret 2016; Pausas et al. 2016). Further research is also required for unraveling the legacy effect of drought on the vascular system of plants (Anderegg et al. 2013, 2015a) and how allocation to roots, stems, and leaves varies under drought conditions (Wolfe et al. 2016).

SUMMARY

We have come a long way in the understanding of plant hydraulics. Fortunately, despite the inherent challenges of investigating liquid water in a metastable state, we have the knowledge, tools and techniques to detect and control for artifacts. The increasing variety of methods available allows cross-checking of experimental VCs and evaluation against intact plants. There is no "holy grail" of methods for embolism detection: all have their advantages and limitations. Importantly, there are many areas of general agreement, starting with the validity of the cohesion-tension mechanism itself, cavitation by air-seeding and the role of pit membranes, VCs in short-conduit species (i.e., all conifers and lots of diffuse-porous angiosperms), the importance of refilling by xylem pressure, many aspects of freezing-related cavitation, the coordination between stomatal regulation and cavitation-avoidance, and the association between cavitation resistance, species ecology, and drought mortality. The functioning of the xylem does indeed form a backbone of plant physiology, because so many functions depend on a viable transpiration stream.

Some of the outstanding problems to be solved include the true vulnerability of large-vesseled angiosperms. Ring-porous trees, lianas, root systems typically have very large vessels, and it is critical to establish their functional properties as convincingly as has already been done for smaller-conduit species. The existence and biological importance of refilling against xylem pressure has yet to be established despite considerable effort. The importance of extra-xylary tissues in controlling leaf- and whole-plant hydraulics is another controversial topic. Pit membranes and end-walls are crucially important structures, controlling both vulnerability to cavitation and influencing hydraulic efficiency. Their structure-and-function in terms of development, chemistry and biomechanics is insufficiently known. We are still far from being able to predict a plant's VC simply from its xylem structure. The linkage between plant hydraulics and stomatal regulation may prove to be a useful modeling tool, but any underlying mechanism for optimizing gas exchange under hydraulic constraints is poorly understood. Finally, genetics and molecular biology underlying the VC phenotype is a huge opportunity for ground-breaking research.

ACKNOWLEDGEMENTS

We are thankful to Amanda Schoonmaker, Brendan Choat, Juan Antonio Martín, Lenka Plavcová and Ryan Stanfield for generously allowing us to use their photographs. Funding was provided by National Science Foundation grant IOS-1450560.

REFERENCES

Alder NN, Pockman WT, Sperry JS, Nuismer S (1997) Use of centrifugal force in the study of xylem cavitation. **J Exp Bot** 48: 665–674

Allen C, Macalady A, Chenchouni H, Bachelet D, McDowell N, Vennetier M, Kitzberger T, Rigling A, Breshears DEH, Gonzalez P, Fensham R, Zhang Z, Castro J, Demidova N, Lim JH, Allard G, Running SW, Semerci A, Cobb N (2010) A global overview of drought and heat-induced tree mortality reveals emerging climate change risks for forests. **For Ecol Manage** 259: 660–684

Almeida-Rodriguez AM, Hacke UG (2012) Cellular localization of aquaporin mRNA in hybrid poplar stems. **Am J Bot** 99: 1249–1254

Anderegg WR, Schwalm C, Biondi F, Camarero JJ, Koch G, Litvak M, Ogle K, Shaw JD, Shevliakova E, Williams A (2015a) Pervasive drought legacies in forest ecosystems and their implications for carbon cycle models. **Science** 349: 528–532

Anderegg WRL (2015) Spatial and temporal variation in plant hydraulic traits and their relevance for climate change impacts on vegetation. **New Phytol** 205: 1008–1014

Anderegg WRL, Berry JA, Smith DD, Sperry JS, Anderegg LDL, Field CB (2012) The roles of hydraulic and carbon stress in a widespread climate-induced forest die-off. **Proc Natl Acad Sci USA** 109: 233–237

Anderegg WRL, Flint A, Huang C, Flint L, Berry JA, Davis F, Sperry JS, Field CB (2015b) Tree mortality predicted from drought-induced vascular damage. **Nat Geosci** 8: 367–371

Anderegg WRL, Klein T, Bartlett M, Sack L, Pellegrini B, Choat B, Jansen S (2016) Meta-analysis reveals that hydraulic traits explain cross-species patterns of drought-induced tree mortality across the globe. **Proc Natl Acad Sci USA** 113: 5024–5029

Anderegg WRL, Placova L, Anderegg LDL, Hacke UG, Berry JA, Field CB (2013) Drought's legacy: Hydraulic deterioration underlies widespread aspen die-off and portends increased future vulnerability. **Global Change Biol** 19: 1188–1196

Aranda I, Gil-Pelegrín E, Gascó A, Guevara MA, Cano JF, De Miguel M, Ramírez-Valiente JA, Peguero-Pina JJ, Perdiguero P, Soto A, Cervera MT, Collada C (2012) Drought response in forest trees: From the species to the gene. In: Aroca R, ed. *Plant Responses to Drought Stress: From Morphological to Molecular Features*. Springer Berlin Heidelberg, Berlin, Heidelberg. pp. 293–333

Aspinwall MJ, King JS, Domec JC, McKeand SE, Isik F (2011) Genetic effects on transpiration, canopy conductance, stomatal sensitivity to vapour pressure deficit, and cavitation resistance in loblolly pine. **Ecohydrology** 4: 168–182

Baert A, De Schepper V, Steppe K (2015) Variable hydraulic resistances and their impact on plant drought response modelling. **Tree Physiol** 35: 439–449

Balfour DA, Midgley JJ (2006) Fire induced stem death in an African acacia is not caused by canopy scorching. **Austral Ecol** 31: 892–896

Ball MC, Canny MJ, Huang CX, Egerton JJG, Wolfe J (2006) Freeze/thaw-induced embolism depends on nadir temperature: The heterogeneous hydration hypothesis. **Plant Cell Environ** 29: 729–745

Beikircher B, Mayr S (2015) Avoidance of harvesting and sampling artefacts in hydraulic analyses: A protocol tested on *Malus domestica*. **Tree Physiol** 36: 797–803

Borghetti M, Edwards WrN, Grace J, Jarvis PG, Raschi A (1991) The refilling of embolized xylem in *Pinus sylvestris*. **Plant Cell Environ** 14: 357–369

Bouche PS, Jansen S, Sabalera JC, Cochard H, Burlett R, Delzon S (2016) Low intra-tree variability in resistance to embolism in four Pinaceae species. **Ann For Sci** 73: 681–689

Bouche PS, Larter M, Domec JC, Burlett R, Gasson P, Jansen S, Delzon S (2014) A broad survey of hydraulic and mechanical safety in the xylem of conifers. **J Exp Bot** 65: 4419–4431

Brasier CM (2000) Intercontinental spread and continuing evolution of Dutch elm disease pathogens. In: Dunn CP, ed. *The Elms: Breeding, Conservation, and Disease Management*. Kluwer Academic Publishers, Boston. pp. 61–72

Breshears DD, Cobb NS, Rich PM, Price KP, Allen CD, Balice RG, Romme WH, Kastens JH, Floyd ML, Belnap J (2005) Regional vegetation die-off in response to global-change-type drought. **Proc Natl Acad Sci USA** 102: 15144–15148

Briggs LJ (1950) Limiting negative pressure of water. **J Appl Phys** 21: 721–722

Brodersen C, McElrone AJ (2013) Maintenance of xylem network transport capacity: A review of embolism repair in vascular plants. **Front Plant Sci** 4: 108

Brodersen C, McElrone AJ, Choat B, Matthews MA, Shackel KA (2010) The dynamics of embolism repair in xylem: *In vivo* visualizations using high-resolution computed tomography. **Plant Physiol** 154: 1088–1095

Brodersen CR, Choat B, Chatelet DS, Shackel KA, Matthews MA, McElrone AJ (2013) Xylem vessel relays contribute to radial connectivity in grapevine stems (*Vitis vinifera* and *V. arizonica*; Vitaceae). **Am J Bot** 100: 314–321

Brodersen CR, Lee EF, Choat B, Jansen S, Phillips RJ, Shackel KA, McElrone AJ, Matthews MA (2011) Automated analysis of three-dimensional xylem networks using high-resolution computed tomography. **New Phytol** 191: 1168–1179

Brodribb TJ (2009) Xylem hydraulic physiology: The functional backbone of terrestrial plant productivity. **Plant Sci** 177: 245–251

Brodribb TJ, Bienaimé D, Marmottant P (2016) Revealing catastrophic failure of leaf networks under stress. **Proc Natl Acad Sci USA** 113: 4865–4869

Brodribb TJ, Holbrook NM (2005) Water stress deforms tracheids peripheral to the leaf vein of a tropical conifer. **Plant Physiol** 137: 1139–1146

Brown HR (2013) The theory of the rise of sap in trees: Some historical and conceptual remarks. **Phys Perspect** 15: 320–358

Buckley TN, Mott KA (2013) Modelling stomatal conductance in response to environmental factors. **Plant Cell Environ** 36: 1691–1699

Buckley TN, Sack L, Farquhar GD (2017) Optimal plant water economy. **Plant Cell Environ** 40: 881–896

Cai J, Li S, Zhang H, Zhang S, Tyree MT (2014) Recalcitrant vulnerability curves: Methods of analysis and the concept of fibre bridges for enhanced cavitation resistance. **Plant Cell Environ** 37: 35–44

Canny MJ (1997) Vessel contents during transpiration — Embolisms and refilling. **Am J Bot** 84: 1223–1230

Carlquist S (1985) Observations on functional wood histology of vines and lianas: Vessel dimorphism, tracheids, vasicentric tracheids, narrow vessels, and parenchyma. **Aliso** 11: 139–157

Charrier G, Charra-Vaskou K, Kasuga J, Cochard H, Mayr S, Améglio T (2014) Freeze-thaw stress: Effects of temperature on hydraulic conductivity and ultrasonic activity in ten woody angiosperms. **Plant Physiol** 164: 992–998

Chaumont F, Tyerman SD (2014) Aquaporins: Highly regulated channels controlling plant water relations. **Plant Physiol** 164: 1600–1618

Choat B, Ball M, Luly J, Holtum J (2003) Pit membrane porosity and water stress-induced cavitation in four co-existing dry rainforest tree species. **Plant Physiol** 131: 41–48

Choat B, Brodersen CR, McElrone AJ (2015) Synchrotron X-ray microtomography of xylem embolism in *Sequoia sempervirens* saplings during cycles of drought and recovery. **New Phytol** 205: 1095–1105

Choat B, Brodie TW, Cobb AR, Zwieniecki MA, Holbrook NM (2006) Direct measurements of intervessel pit membrane hydraulic resistance in two angiosperm tree species. **Am J Bot** 93: 993–1000

Choat B, Jansen S, Brodribb TJ, Cochard H, Bhaskar R, Bucci SJ, Delzon S, Feild TS, Gleason S, Jacobson AL, Lens F, Maherali H, Martinez-Vilalta J, Mayr S, Mencuccini M, Mitchell PJ, Nardini A, Pittermann J, Pratt RB, Sperry JS, Westoby M, Wright IJ, Zanne A (2012) Global convergence in the vulnerability of forests to drought. **Nature** 491: 752–755

Choat B, Jansen S, Zwieniecki MA, Smets E, Holbrook NM (2004) Changes in pit membrane porosity due to deflection and stretching: The role of vestured pits. **J Exp Bot** 55: 1569–1575

Christensen-Dalsgaard KK, Tyree MT, Mussone PG (2011) Surface tension phenomena in the xylem sap of three diffuse porous temperate tree species. **Tree Physiol** 31: 361–368

Christman MA, Sperry JS (2010) Single vessel flow measurements indicate scalariform perforation plates confer higher resistance to flow than previously estimated. **Plant Cell Environ** 33: 431–443

Christman MA, Sperry JS, Adler FR (2009) Testing the rare pit hypothesis in three species of *Acer*. **New Phytol** 182: 664–674

Christman MA, Sperry JS, Smith DD (2012) Rare pits, large vessels, and extreme vulnerability to cavitation in a ring-porous tree species. **New Phytol** 193: 713–720

Cochard H, Badel E, Herbette S, Delzon S, Choat B, Jansen S (2013) Methods for measuring plant vulnerability to cavitation: A critical review. **J Exp Bot** 64: 4779–4791

Cochard H, Bodet C, Ameglio T, Cruiziat P (2000) Cryo-scanning electron microscopy observations of vessel content during transpiration in walnut petioles: facts or artifacts? **Plant Physiol** 124: 1191–1202

Cochard H, Cruiziat P, Tyree MT (1992) Use of positive pressures to establish vulnerability curves: Further support for the air-seeding hypothesis and implications for pressure-volume analysis. **Plant Physiol** 100: 205–209

Cochard H, Delzon S (2013) Hydraulic failure and repair are not routine in trees. **Ann Sci For** 70: 659–661

Cochard H, Ewers FW, Tyree MT (1994) Water relations of a tropical vine-like bamboo (*Rhipidocladum racemiflorum*): Root pressures, vulnerability to cavitation and seasonal changes in embolism. **J Exp Bot** 45: 1085–1089

Cochard H, Froux F, Mayr S, Coutand C (2004) Xylem wall collapse in water-stressed pine needles. **Plant Physiol** 134: 401–408

Cochard H, Gaelle D, Bodet C, Tharwat I, Poirier M, Ameglio T (2005) Evaluation of a new centrifuge technique for rapid generation of xylem vulnerability curves. **Physiol Plant** 124: 410–418

Cochard H, Herbette S, Barigah T, Vilagrosa A (2010) Does sample length influence the shape of vulnerability to cavitation curves? A test with the Cavitron spinning technique. **Plant Cell Environ** 33: 1543–1552

Cochard H, Holtta T, Herbette S, Delzon S, Mencuccini M (2009) New insights into the mechanisms of water-stress-induced cavitation in conifers. **Plant Physiol** 151: 949–954

Corcuera L, Cochard H, Gil-Pelegrin E, Notivol E (2011) Phenotypic plasticity in mesic populations of *Pinus pinaster* improves resistance to xylem embolism (P50) under severe drought. **Trees** 25: 1033–1042

Cowan IR, Farquhar GD (1977) Stomatal function in relation to leaf metabolism and environment. In: Jennings DH, ed. *Integration of Activity in the Higher Plant*. Cambridge University Press, Cambridge. pp. 471–505

Crombie DS, Hipkins MF, Milburn JA (1985) Gas penetration of pit membranes in the xylem of *Rhododendron* as the cause of acoustically detectable sap cavitation. **Aust J Plant Physiol** 12: 445–454

Davis SD, Sperry JS, Hacke UG (1999) The relationship between xylem conduit diameter and cavitation caused by freezing. **Am J Bot** 86: 1367–1372

De Rybel B, Mähönen AP, Helariutta Y, Weijers D (2016) Plant vascular development: From early specification to differentiation. **Nat Rev Mol Cell Biol** 17: 30–40

Delzon S, Cochard H (2014) Recent advances in tree hydraulics highlight the ecological significance of the hydraulic safety margin. **New Phytol** 203: 355–358

Delzon S, Douthe C, Sala A, Cochard H (2010) Mechanism of water-stress induced cavitation in conifers: Bordered pit structure and function support the hypothesis of seal capillary-seeding. **Plant Cell Environ** 33: 2101–2111

Dixon HH (1914) *Transpiration and the Ascent of Sap*. Macmillan and Co. Ltd., London

Dixon HH, Joly J (1895) On the ascent of sap. **Philos Trans R Soc Lond Ser B: Biol Sci** 186: 563–576

Ducrey M, Duhoux F, Huc R, Rigolot E (1996) The ecophysiological and growth responses of Aleppo pine (*Pinus halepensis*) to controlled heating applied to the base of the trunk. **Can J For Res** 26: 1366–1374

Ennajeh M, Nouiri M, Khemira H, Cochard H (2011) Improvement to the air-injection technique to estimate xylem vulnerability to cavitation. **Trees** 25: 705–710

Farquhar G, von Caemmerer Sv, Berry J (1980) A biochemical model of photosynthetic CO2 assimilation in leaves of C3 species. **Planta** 149: 78–90

Fleury D, Jefferies S, Kuchel H, Langridge P (2010) Genetic and genomic tools to improve drought tolerance in wheat. **J Exp Bot** 61: 3211–3222

Gasco A, Nardini A, Gortan E, Salleo S (2006) Ion-mediated increase in the hydraulic conductivity of Laurel stems: Role of pits and consequences for the impact of cavitation on water transport. **Plant Cell Environ** 29: 1946–1955

Giordano R, Salleo A, Salleo S, Wanderlingh F (1978) Flow in xylem vessels and Poiseuille's law. **Can J Bot** 56: 333–338

Gleason SM, Westoby M, Jansen S, Choat B, Hacke UG, Pratt RB, Bhaskar R, Brodribb TJ, Bucci SJ, Cao KF, Cochard H, Delzon S, Domec JC, Fan ZX, Feild TS, Jacobsen AL, Johnson DM, Lens F, Maherali H, Martinez-Vilalta J, Mayr S, McCulloh KA, Mencuccini M, Mitchell PJ, Morris H, Nardini A, Pittermann J, Plavcova L, Schreiber SG, Sperry JS, Wright IJ, Zanne AE (2015) Weak tradeoff between xylem safety and xylem-specific hydrualic efficiency across the world's woody plant species. **New Phytol** 209: 123–136

Granier A (1985) Une nouvelle methode pour la mesure du flux de seve brute le tronc des arbres. **Ann Sci For** 42: 193–200

Hacke U, Sauter JJ (1996) Xylem dysfunction during winter and recovery of hydraulic conductivity in diffuse-porous and ring-porous trees. **Oecologia** 105: 435–439

Hacke UG, Laur J (2016) Aquaporins: Channels for the molecule of life. **eLS**: DOI: 10.1002/9780470015902.a9780470001289.pub9780470015902

Hacke UG, Plavcová L, Almeida-Rodriguez A, King-Jones S, Zhou W, Cooke JE (2010) Influence of nitrogen fertilization on xylem traits and aquaporin expression in stems of hybrid poplar. **Tree Physiol** 30: 1016–1025

Hacke UG, Sperry JS (2001) Functional and ecological xylem anatomy. **Perspect Plant Ecol Evol Syst** 4: 97–115

Hacke UG, Sperry JS, Pittermann J (2004) Analysis of circular bordered pit function II. Gymnosperm tracheids with torus-margo pit membranes. **Am J Bot** 91: 386–400

Hacke UG, Sperry JS, Pockman WP, Davis SD, McCulloh KA (2001a) Trends in wood density and structure are linked to prevention of xylem implosion by negative pressure. **Oecologia** 126: 457–461

Hacke UG, Sperry JS, Wheeler JK, Castro L (2006) Scaling of angiosperm xylem structure with safety and efficiency. **Tree Physiol** 26: 689–701

Hacke UG, Spicer R, Schreiber SG, Plavcová L (2017) An ecophysiological and developmental perspective on variation in vessel diameter. **Plant Cell Environ** 40: 831–845

Hacke UG, Stiller V, Sperry JS, Pittermann J, McCulloh KA (2001b) Cavitation fatigue: Embolism and refilling cycles can weaken cavitation resistance of xylem. **Plant Physiol** 125: 779–786

Hacke UG, Venturas MD, MacKinnon ED, Jacobsen AL, Sperry JS, Pratt RB (2015) The standard centrifuge method accurately measures vulnerability curves of long-vesselled olive stems. **New Phytol** 205: 116–127

Hao GY, Lucero ME, Sanderson SC, Zacharias EH, Holbrook NM (2013) Polyploidy enhances the occupation of heterogeneous environments through hydraulic related trade-offs in *Atriplex canescens* (Chenopodiaceae). **New Phytol** 197: 970–978

Haynes WM (2014) *CRC Handbook of Chemistry and Physics*. CRC press, Boca Raton, Florida

Hietz P, Rosner S, Sorz J, Mayr S (2008) Comparison of methods to quantify loss of hydraulic conductivity in Norway spruce. **Ann For Sci** 65: 502

Hillabrand RM, Hacke UG, Lieffers VJ (2016) Drought-induced xylem pit membrane damage in aspen and balsam poplar. **Plant Cell Environ** 39: 2210−2220

Holbrook NM, Ahrens ET, Burns MJ, Zwieniecki MA (2001) *In vivo* observation of cavitation and embolism repair using magnetic resonance imaging. **Plant Physiol** 126: 27−31

Holbrook NM, Zwieniecki MA (1999) Embolism repair and xylem tension: Do we need a miracle? **Plant Physiol** 120: 7−10

Hubbard RM, Rhoades CC, Elder K, Negron J (2013) Changes in transpiration and foliage growth in lodgepole pine trees following mountain pine beetle attack and mechanical girdling. **For Ecol Manage** 289: 312−317

Jacobsen AL, Ewers FW, Pratt RB, Paddock WA, Davis SD (2005) Do xylem fibers affect vessel cavitation resistance? **Plant Physiol** 139: 546−556

Jacobsen AL, Pratt RB (2012) No evidence for an open vessel effect in centrifuge-based vulnerability curves of a long-vesselled liana (*Vitis vinifera*). **New Phytol** 194: 982−990

Jacobsen AL, Pratt RB, Davis SD, Tobin MF (2014) Geographic and seasonal variation in chaparral vulnerability to cavitation. **Madrono** 61: 317−327

Jacobsen AL, Pratt RB, Ewers FW, Davis SD (2007) Cavitation resistance among 26 chaparral species of southern California. **Ecol Monogr** 77: 99−115

Jacobsen AL, Pratt RB, Tobin MF, Hacke UG, Ewers FW (2012) A global analysis of xylem vessel length in woody plants. **Am J Bot** 99: 1583−1591

Jacobsen AL, Rodriguez-Zaccaro FD, Lee TF, Valdovinos J, Toschi HS, Martinez JA, Pratt RB (2015) Grapevine xylem development, architecture, and function. In: Hacke UW, ed. *Functional and Ecological Xylem Anatomy*. Springer, Cham, Heidelberg, New York. pp. 133–162

Jacobsen AL, Tobin MF, Toschi HS, Percolla MI, Pratt RB (2016) Structural determinants of increased susceptibility to dehydration-induced cavitation in post-fire resprouting chaparral shrubs. **Plant Cell Environ** 39: 2473–2485

Jansen S, Choat B, Pletsers A (2009) Morphological variation in intervessel pit membranes and implications to xylem function in angiosperms. **Am J Bot** 96: 409–419

Jansen S, Lamy JB, Burlett R, Cochard H, Gasson P, Delzon S (2012) Plasmodesmatal pores in the torus of bordered pit membranes affect cavitation resistance of conifer xylem. **Plant Cell Environ** 35: 1109–1120

Jarbeau JA, Ewers FW, Davis SD (1995) The mechanism of water-stress-induced embolism in two species of chaparral shrubs. **Plant Cell Environ** 18: 189–196

Jones HG, Sutherland R (1991) Stomatal control of xylem embolism. **Plant Cell Environ** 14: 607–612

Jordan CF, Kline JR (1977) Transpiration of trees in a tropical rainforest. **J Appl Ecol**: 853–860

Kikuta SB, Lo Gullo MA, Nardini A, Richter H, Salleo S (1997) Ultrasound acoustic emissions from dehydrating leaves of deciduous and evergreen trees. **Plant Cell Environ** 20: 1381–1390

Kitin P, Voelker SL, Meinzer FC, Beeckman H, Strauss SH, Lachenbruch B (2010) Tyloses and phenolic deposits in xylem vessels impede water transport in low-lignin transgenic poplars: A study by cryo-fluorescence microscopy. **Plant Physiol** 154: 887–898

Knipfer T, Cuneo IF, Brodersen CR, McElrone AJ (2016) *In situ* visualization of the dynamics in xylem embolism formation and removal in the absence of root pressure: A study on excised grapevine stems. **Plant Physiol** 171: 1024–1036

Koch GW, Sillett SC, Jennings GM, Davis SD (2004) The limits to tree height. **Nature** 428: 851–854

Kolb KJ, Sperry JS (1999a) Differences in drought adaptation between subspecies of sagebrush (*Artemisia tridentata*). **Ecology** 80: 2373–2384

Kolb KJ, Sperry JS (1999b) Transport constraints on water use by the Great Basin shrub, *Artemisia tridentata*. **Plant Cell Environ** 22: 925–935

Kolb KJ, Sperry JS, Lamont BB (1996) A method for measuring xylem hydraulic conductance and embolism in entire root and shoot systems. **J Exp Bot** 47: 1805–1810

Kukowski K, Schwinning S, Schwartz B (2013) Hydraulic responses to extreme drought conditions in three co-dominant tree species in shallow soil over bedrock. **Oecologia** 171: 819–830

Kuroda K (1991) Mechanism of cavitation development in the pine wilt disease. **Eur J For Pathol** 21: 82–89

Lamy JB, Bouffier L, Burlett R, Plomion C, Cochard H, Delzon S (2011) Uniform selection as a primary force reducing population genetic differentiation of cavitation resistance across a species range. **PLoS ONE** 6: e23476

Lamy JB, Delzon S, Bouche PS, Alia R, Vendramin GG, Cochard H, Plomion C (2014) Limited genetic variability and phenotypic plasticity detected for cavitation resistance in a Mediterranean pine. **New Phytol** 201: 874–886

Langan S, Ewers FW, Davis SD (1997) Xylem dysfunction caused by water stress and freezing in two species of co-occurring chaparral shrubs. **Plant Cell Environ** 20: 425–437

Lens F, Sperry JS, Christman MA, Choat B, Rabaey D, Jansen S (2010) Testing hypotheses that link wood anatomy to cavitation resistance and hydraulic conductivity in the genus *Acer*. **New Phytol** 190: 709–723

Lersten NR (1997) Occurrence of endodermis with a casparian strip in stem and leaf. **Bot Rev** 63: 265–272

Lewis AM (1988) A test of the air-seeding hypothesis using *Sphagnum* hyalocysts. **Plant Physiol** 87: 577–582

Lewis AM, Boose ER (1995) Estimating volume flow rates through xylem conduits. **Am J Bot** 82: 1112–1116

Li M, López R, Venturas MD, Martín JA, Domínguez J, Gordaliza G, Gil L, Rodríguez-Calcerrada J (2016) Physiological and biochemical differences among *Ulmus minor* genotypes showing a gradient of resistance to Dutch elm disease. **For Pathol** 46: 215–228

Li S, Assmann SM, Albert R (2006) Predicting essential components of signal transduction networks: A dynamic model of guard cell abscisic acid signaling. **PLoS Biol** 4: e312

Li Y, Sperry JS, Bush SE, Hacke UG (2008) Evaluation of centrifugal methods for measuring xylem cavitation in conifers, diffuse- and ring-porous angiosperms. **New Phytol** 177: 558–568

Lintunen A, Hölttä T, Kulmala M (2013) Anatomical regulation of ice nucleation and cavitation helps trees to survive freezing and drought stress. **Sci Rep** 3: 2031

Loepfe L, Martinez-Vilalta J, Pinol J, Mencuccini M (2007) The relevance of xylem network structure for plant hydraulic efficiency and safety. **J Theor Biol** 247: 788–803

López R, Cano FJ, Choat B, Cochard H, Gil L (2016) Plasticity in vulnerability to cavitation of *Pinus canariensis* occurs only at the driest end of an aridity gradient. **Front Plant Sci** 7: 769

López R, de Heredia UL, Collada C, Cano FJ, Emerson BC, Cochard H, Gil L (2013) Vulnerability to cavitation, hydraulic efficiency, growth and survival in an insular pine (*Pinus canariensis*). **Ann Bot** 111: 1167–1179

Lucas WJ, Groover A, Lichtenberger R, Furuta K, Yadav SR, Helariutta Y, He XQ, Fukuda H, Kang J, Brady SM (2013) The plant vascular system: Evolution, development and functions. **J Integr Plant Biol** 55: 294–388

Mackay DS, Roberts DE, Ewers BE, Sperry JS, McDowell N, Pockman W (2015) Interdependence of chronic hydraulic dysfunction and canopy processes can improve integrated models of tree response to drought. **Water Resour Res** 51: 6156–6176

Maherali H, Walden AE, Husband BC (2009) Genome duplication and the evolution of physiological responses to water stress. **New Phytol** 184: 721–731

Marshall D (1958) Measurement of sap flow in conifers by heat transport. **Plant Physiol** 33: 385–396

Martin-StPaul N, Longepierre D, Huc R, Delzon S, Burlett R, Joffre R, Rambal S, Cochard H (2014) How reliable are methods to assess xylem vulnerability to cavitation? The issue of 'open vessel' artifact in oaks. **Tree Physiol** 34: 894–905

Martín JA, Solla A, Esteban LG, de Palacios P, Gil L (2009) Bordered pit and ray morphology involvement in elm resistance to *Ophiostoma novo-ulmi*. **Can J For Res** 39: 420–429

Martín JA, Solla A, Ruiz-Villar M, Gil L (2013) Vessel length and conductivity of *Ulmus* branches: Ontogenetic changes and relation to resistance to Dutch elm disease. **Trees** 27: 1239–1248

Martín JA, Solla A, Woodward S, Gil L (2007) Detection of differential changes in lignin composition of elm xylem tissues inoculated with *Ophiostoma novo-ulmi* using Fourier transform-infrared spectroscopy. **For Pathol** 37: 187–191

Martínez-Vilalta J, Lloret F (2016) Drought-induced vegetation shifts in terrestrial ecosystems: The key role of regeneration dynamics. **Global Planet Change** 144: 94–108

Mayr S, Gruber A, Bauer H (2003a) Repeated freeze-thaw cycles induce embolism in drought stressed conifers (Norway spruce, stone pine). **Planta** 217: 436–441

Mayr S, Schwienbacher F, Bauer H (2003b) Winter at the alpine timberline. Why does embolism occur in Norway spruce but not in stone pine? **Plant Physiol** 131: 780–792

Mayr S, Sperry JS (2010) Freeze-thaw induced embolism in *Pinus contorta*: Centrifuge experiments validate the "thaw-expansion" hypothesis but conflict with ultrasonic data. **New Phytol** 18: 1016–1024

Mayr S, Zublasing V (2010) Ultrasonic emissions from conifer xylem exposed to repeated freezing. **Plant Physiol** 167: 34–40

McCulloh KA, Sperry JS, Lachenbruch B, Meinzer FC, Reich PB, Voelker S (2010) Moving water well: Comparing hydraulic efficiency in twigs and trunks of coniferous, ring-porous, and diffuse-porous saplings from temperate and tropical forests. **New Phytol** 186: 439–450

McCully ME (1999) Root xylem embolisms and refilling. Relation to water potentials of soil, roots, and leaves, and osmotic potentials of root xylem sap. **Plant Physiol** 119: 1001–1008

McDowell N, Fisher RA, Xu C, Domec JC, Holtta T, Mackay DS, Sperry JS, Boutz A, Diskman L, Geheres N, Limousin JM, Macalady A, Martinez-Vilalta J, Mencuccini M, Plaut J, Ogee J, Pangle R, Rasse DP, Ryan MG, Sevanto S, Waring RH, Williams AP, Yepez EA, Pockman WT (2013) Evaluating theories of drought-induced vegetation mortality using a multimodel-experimental framework. **New Phytol** 200: 304–321

Melcher PJ, Zwieniecki MA, Holbrook NM (2003) Vulnerability of xylem vessels to cavitation in sugar maple. Scaling from individual vessels to whole branches. **Plant Physiol** 131: 1775–1780

Ménard D, Pesquet E (2015) Cellular interactions during tracheary elements formation and function. **Curr Opin Plant Biol** 23: 109–115

Mercury L, Shmulovich KI (2014) Experimental superheating and cavitation of water and solutions at spinodal-like negative pressures. In: Mercury L, Tas N, Zilberbrand M, eds. *Transport and Reactivity of Solutions in Confined Hydrosystems. NATO Science for Peace and Security Series C: Environmental Security*. Springer, Dordrecht. pp. 159–171

Michaletz ST, Johnson E, Tyree M (2012) Moving beyond the cambium necrosis hypothesis of post-fire tree mortality: Cavitation and deformation of xylem in forest fires. **New Phytol** 194: 254–263

Milburn JA (1973) Cavitation in *Ricinus* by acoustic detection: Induction in excised leaves by various factors. **Planta** 110: 253–265

Mishima O, Stanley HE (1998) The relationship between liquid, supercooled and glassy water. **Nature** 396: 329–335

Münch E (1927) Versuche über den Saftkreislauf. **Berichte der Deutschen Botanischen Gesellschaft** 45: 340–346

Murakami Y, Funada R, Sano Y, Ohtani J (1999) The differentiation of contact cells and isolation cells in the xylem ray parenchyma of *Populus maximowiczii*. **Ann Bot** 84: 429–435

Nardini A, Gascò A, Trifilò P, Gullo MAL, Salleo S (2007) Ion-mediated enhancement of xylem hydraulic conductivity is not always suppressed by the presence of Ca^{2+} in the sap. **J Exp Bot** 58: 2609–2615

Nardini A, LoGullo MA, Salleo S (2011) Refilling embolized xylem conduits: Is it a matter of phloem unloading? **Plant Sci** 180: 604–611

Nardini A, Savi T, Losso A, Petit G, Pacilè S, Tromba G, Mayr S, Trifilò P, Lo Gullo MA, Salleo S (2017) X-ray microtomography observations of xylem embolism in stems of *Laurus nobilis* are consistent with hydraulic measurements of percentage loss of conductance. **New Phytol** 213: 1068–1075

Newbanks D, Bosch A, Zimmermann MH (1983) Evidence for xylem dysfunction by embolization in Dutch elm disease. **Phytopathology** 73: 1060–1063

Nobel PS (1991) Achievable productivities of certain CAM plants: Basis for high values compared with C-3 and C-4 plants. **New Phytol** 119: 183–206

North GB, Nobel PS (1997) Root-soil contact for the desert succulent *Agave deserti* in wet and drying soil. **New Phytol** 135: 21–29

North GB, Nobel PS (1998) Water uptake and structural plasticity along roots of a desert succulent during prolonged drought. **Plant Cell Environ** 21: 705–713

Oda Y, Fukuda H (2014) Emerging roles of small GTPases in secondary cell wall development. **Front Plant Sci** 5: 428

Ogasa MY, Utsumi Y, Miki NH, Yazaki K, Fukuda K (2016) Cutting stems before relaxing xylem tension induces artefacts in *Vitis coignetiae*, as evidenced by magnetic resonance imaging. **Plant Cell Environ** 39: 329–337

Pammenter Nv, Van der Willigen C (1998) A mathematical and statistical analysis of the curves illustrating vulnerability of xylem to cavitation. **Tree Physiol** 18: 589–593

Pausas JG, Pratt RB, Keeley JE, Jacobsen AL, Ramirez AR, Vilagrosa A, Paula S, Kaneakua-Pia IN, Davis SD (2016) Towards understanding resprouting at the global scale. **New Phytol** 209: 945–954

Pereira L, Bittencourt PR, Oliveira RS, Junior M, Barros FV, Ribeiro RV, Mazzafera P (2016) Plant pneumatics: Stem air flow is related to embolism-new perspectives on methods in plant hydraulics. **New Phytol** 211: 357–370

Pérez-Donoso AG, Greve LC, Walton JH, Shackel KA, Labavitch JM (2007) *Xylella fastidiosa* infection and ethylene exposure result in xylem and water movement disruption in grapevine shoots. **Plant Physiol** 143: 1024–1036

Pérez-Donoso AG, Sun Q, Roper MC, Greve LC, Kirkpatrick B, Labavitch JM (2010) Cell wall-degrading enzymes enlarge the pore size of intervessel pit membranes in healthy and *Xylella fastidiosa*-infected grapevines. **Plant Physiol** 152: 1748–1759

Pfautsch S, Hölttä T, Mencuccini M (2015a) Hydraulic functioning of tree stems—Fusing ray anatomy, radial transfer and capacitance. **Tree Physiol** 35: 706–722

Pfautsch S, Renard J, Tjoelker MG, Salih A (2015b) Phloem as capacitor: Radial transfer of water into xylem of tree stems occurs via symplastic transport in ray parenchyma. **Plant Physiol** 167: 963–971

Pickard WF (1981) The ascent of sap in plants. **Prog Biophys Mol Biol** 37: 181–229

Piñol J, Sala A (2000) Ecological implications of xylem cavitation for several Pinaceae in the pacific Northern USA. **Funct Ecol** 14: 538–545

Pittermann J, Sperry JS (2003) Tracheid diameter is the key trait determining extent of freezing-induced cavitation in conifers. **Tree Physiol** 23: 907–914

Pittermann J, Sperry JS (2006) Analysis of freeze-thaw embolism in conifers: The interaction between cavitation pressure and tracheid size. **Plant Physiol** 140: 374–382

Pittermann J, Sperry JS, Hacke UG, Wheeler JK, Sikkema EH (2005) Torus-margo pits help conifers compete with angiosperms. **Science** 310: 1924

Pittermann J, Sperry JS, Hacke UG, Wheeler JK, Sikkema EH (2006a) Inter-tracheid pitting and the hydraulic efficiency of conifer wood: The role of tracheid allometry and cavitation protection. **Am J Bot** 93: 1105–1113

Pittermann J, Sperry JS, Wheeler JK, Hacke UG, Sikkema EH (2006b) Mechanical reinforcement of tracheids compromises the hydraulic efficiency of conifer xylem. **Plant, Cell Environ** 29: 1618–1628

Pivovaroff AL, Burlett R, Lavigne B, Cochard H, Santiago LS, Delzon S (2016) Testing the 'microbubble effect' using the Cavitron technique to measure xylem water extraction curves. **AoB Plants** 8: plw011

Pivovaroff AL, Sack L, Santiago LS (2014) Coordination of stem and leaf hydraulic conductance in southern California shrubs: A test of the hydraulic segmentation hypothesis. **New Phytol** 203: 842–850

Plavcová L, Hacke UG (2011) Heterogeneous distribution of pectin epitopes and calcium in different pit types of four angiosperm species. **New Phytol** 192: 885–897

Plavcova L, Hacke UG, Almeida-Rodriguez AM, Li E, Douglas CJ (2013) Gene expression patterns underlying changes in xylem structure and function in response to increased nitrogen availability in hybrid poplar. **Plant Cell Environ** 36: 186–199

Plavcová L, Hacke UG, Sperry JS (2011) Linking irradiance-induced changes in pit membrane ultrastructure with xylem vulnerability to cavitation. **Plant Cell Environ** 34: 501–513

Pockman WT, Sperry JS, O'Leary JW (1995) Sustained and significant negative water pressure in xylem. **Nature** 378: 715–716

Poole PH, Sciortino F, Essmann U, Stanley HE (1992) Phase behaviour of metastable water. **Nature** 360: 324–328

Powell T, Galbraith D, Christoffersen B, Harper A, Imbuzeiro H, Rowland L, Almeida S, Brandom P, da Costa A, Costa MaLN, Malhi Y, Saleska S, Sotta E, Williams M, Meir P, Moorcroft P (2013) Confronting model predictions of carbon fluxes with measurements of Amazon forests subjected to experimental drought. **New Phytol** 200: 350–365

Pratt R, MacKinnon E, Venturas M, Crous C, Jacobsen A (2015) Root resistance to cavitation is accurately measured using a centrifuge technique. **Tree Physiol** 35: 185–196

Pratt RB, Jacobsen AL (2017) Conflicting demands on angiosperm xylem: Tradeoffs among storage, transport, and biomechanics. **Plant Cell Environ** 40: 897–913

Pratt RB, Jacobsen AL, Ramirez AR, Helms AM, Traugh CA, Tobin MF, Heffner MS, Davis SD (2014) Mortality of resprouting chaparral shrubs after a fire and during a record drought: Physiological mechanisms and demographic consequences. **Global Change Biol** 20: 893–907

Rice KJ, Matzner SL, Byer W, Brown JR (2004) Patterns of tree dieback in Queensland, Australia: The importance of drought stress and the role of resistance to cavitation. **Oecologia** 139: 190–198

Rockwell FE, Wheeler JK, Holbrook NM (2014) Cavitation and its discontents: Opportunities for resolving current controversies. **Plant Physiol** 164: 1649–1660

Rodríguez-Calcerrada J, Li M, López R, Cano FJ, Oleksyn J, Atkin OK, Pita P, Aranda I, Gil L (2017) Drought-induced shoot dieback starts with massive root xylem embolism and variable depletion of nonstructural carbohydrates in seedlings of two tree species. **New Phytol** 213: 597−610

Rosner S, Klein A, Wimmer R, Karlsson B (2006) Extraction of features from ultrasound acoustic emissions: A tool to assess the hydraulic vulnerability of Norway spruce trunkwood? **New Phytol** 171: 105−116

Rowland L, da Costa ACL, Galbraith DR, Oliviera RS, Binks OJ, Oliveira, AAR, Pullen AM, Doughty CE, Metcalfe DB, Vasconcelos SS, Ferreira LV, Malhi Y, Grace J, Mencuccini M, Meir P (2015) Death from drought in tropical forests is triggered by hydraulics not carbon starvation. **Nature** 528: 119−122

Růžička K, Ursache R, Hejátko J, Helariutta Y (2015) Xylem development-From the cradle to the grave. **New Phytol** 207: 519−535

Ryu J, Hwang BG, Lee SJ (2016) *In vivo* dynamic analysis of water refilling in embolized xylem vessels of intact *Zea mays* leaves. **Ann Bot** 118: 1033–1042

Sack L, Melcher PJ, Zwieniecki MA, Holbrook NM (2002) The hydraulic conductance of the angiosperm leaf lamina: A comparison of three measurement methods. **J Exp Bot** 53: 2177−2184

Sack L, Scoffoni C (2012) Measurement of leaf hydraulic conductance and stomatal conductance and their responses to irradiance and dehydration using the Evaporative Flux Method (EFM). **J Vis Exp** pii: 4179 doi:10.3791/4179

Sack L, Scoffoni C, Johnson DM, Buckley TN, Brodribb TJ (2015) The anatomical determinants of leaf hydraulic function. In: Hacke UW, ed. *Functional and Ecological Xylem Anatomy*. Springer, Cham, Heidelberg, New York. pp. 255−271

Sala A, Piper F, Hoch G (2010) Physiological mechanisms of drought-induced tree mortality are far from being resolved. **New Phytol** 186: 274−281

Salleo S, Hinckley TM, Kikuta SB, Lo Gullo MA, Weilgony P, Yoon TM, Richter H (1992) A method for inducing xylem emboli *in situ*: Experiments with a field-grown tree. **Plant Cell Environ** 15: 491−497

Salleo S, Lo Gullo MA, De Paoli D, Zippo M (1996) Xylem recovery from cavitation-induced embolism in young plants of *Laurus nobilis*: A possible mechanism. **New Phytol** 132: 47−56

Salleo S, Lo Gullo MA, Trifilo P, Nardini A (2004) New evidence for a role of vessel-associated cells and phloem in the rapid xylem refilling of cavitated stems of *Laurus nobilis* L. **Plant Cell Environ** 27: 1065−1076

Salleo S, Trifilo P, Esposito S, Nardini A, LoGullo MA (2009) Starch-to-sugar conversion in wood parenchyma of field-growing *Laurus nobilis* plants: A component of the signal pathway for embolism repair? **Funct Plant Biol** 36: 815−825

Salleo S, Trifilo P, LoGullo MA (2006) Phloem as a possible major determinant of rapid cavitation reversal in *Laurus nobilis* (laurel). **Funct Plant Biol** 33: 1063−1074

Sauter JJ (1984) Detection of embolization of vessels by a double staining technique. **J Plant Physiol** 116: 331−342

Sauter JJ, Iten W, Zimmermann MH (1973) Studies on the release of sugar into the vessels of sugar maple, *Acer saccharum*. **Can J Bot** 51: 1−8

Schenk HJ, Espino S, Romo DM, Nima N, Do AY, Michaud JM, Papahadjopoulos-Sternberg B, Yang J, Zuo YY, Steppe K (2016) Xylem surfactants introduce a new element to the cohesion-tension theory. **Plant Physiol** 173: 1177−1196

Schenk HJ, Steppe K, Jansen S (2015) Nanobubbles: A new paradigm for air-seeding in xylem. **Trends Plant Sci** 20: 199−205

Schlesinger WH, Jasechko S (2014) Transpiration in the global water cycle. **Agric For Meteorol** 189: 115−117

Schreiber SG, Hacke UG, Chamberland S, Lowe CW, Kamelchuk D, Bräutigam K, Campbell MM, Thomas BR (2016) Leaf size serves as a proxy for xylem vulnerability to cavitation in plantation trees. **Plant Cell Environ** 39: 272−281

Schreiber SG, Hacke UG, Hamann A, Thomas BR (2011) Genetic variation of hydraulic and wood anatomical traits in hybrid poplar and trembling aspen. **New Phytol** 190: 150−160

Scoffoni C, Albuquerque C, Brodersen C, Townes SV, John GP, Bartlett MK, Buckley TN, McElrone AJ, Sack L (2017) Outside-xylem vulnerability, not xylem embolism, controls leaf hydraulic decline during dehydration. **Plant Physiol** 173: 1197−1210

Scoffoni C, Sack L (2015) Are leaves 'freewheelin'? Testing for a Wheeler-type effect in leaf xylem hydraulic decline. **Plant Cell Environ** 38: 534−543

Secchi F, Zwieniecki MA (2010) Patterns of PIP gene expression in *Populus trichocarpa* during recovery from xylem embolism suggest a major role for the PIP1 aquaporin subfamily as moderators of the refilling process. **Plant Cell Environ** 33: 1285−1297

Sevanto S, Holbrook NM, Ball MC (2012) Freeze/thaw-induced embolism: Probability of critical bubble formation depends on speed of ice formation. **Front Plant Sci** 3: 107

Sevanto S, McDowell NaDT, Pangle R, Pockman WP (2013) How do trees die? A test of the hydraulic failure and carbon starvation hypotheses. **Plant Cell Environ** 37: 153−161

Sperry JS (1986) Relationship of xylem embolism to xylem pressure potential, stomatal closure, and shoot morphology in the palm *Rhapis excelsa*. **Plant Physiol** 80: 110−116

Sperry JS (2003) Evolution of water transport and xylem structure. **Int J Plant Sci** 164: S115−S127

Sperry JS (2011) Hydraulics of vascular water transport. In: P. W, ed. *Mechanical Integration of Plant Cells and Plants*. Springer-Verlag, Berlin. pp. 303−327

Sperry JS, Adler FR, Campbell GS, Comstock JP (1998) Limitation of plant water use by rhizosphere and xylem conductance: Results from a model. **Plant Cell Environ** 21: 347−359

Sperry JS, Christman MA, Smith DD (2012) Vulnerability curves by centrifugation: Is there an open vessel artifact, and are "r" shaped curves necessarily invalid? **Plant Cell Environ** 35: 601–610

Sperry JS, Donnelly JR, Tyree MT (1988) A method for measuring hydraulic conductivity and embolism in xylem. **Plant Cell Environ** 11: 35–40

Sperry JS, Hacke UG, Pittermann J (2006) Size and function in conifer tracheids and angiosperm vessels. **Am J Bot** 93: 1490–1500

Sperry JS, Hacke UG, Wheeler JK (2005) Comparative analysis of end-wall resistance in xylem conduits. **Plant Cell Environ** 28: 456–465

Sperry JS, Holbrook NM, Zimmermann MH, Tyree MT (1987) Spring filling of xylem vessels in wild grapevine. **Plant Physiol** 83: 414–417

Sperry JS, Love DM (2015) What plant hydraulics can tell us about plant responses to climate-change droughts. **New Phytol** 207: 14–27

Sperry JS, Saliendra NZ (1994) Intra-and inter-plant variation in xylem cavitation in *Betula occidentalis*. **Plant Cell Environ** 17: 1233–1241

Sperry JS, Saliendra NZ, Pockman WT, Cochard H, Cruiziat P, Davis SD, Ewers FW, Tyree MT (1996) New evidence for large negative xylem pressures and their measurement by the pressure chamber method. **Plant Cell Environ** 19: 427–436

Sperry JS, Sullivan JEM (1992) Xylem embolism in response to freeze-thaw cycles and water stress in ring-porous, diffuse-porous, and conifer species. **Plant Physiol** 100: 605–613

Sperry JS, Tyree MT (1988) Mechanism of water stress-induced xylem embolism. **Plant Physiol** 88: 581–587

Sperry JS, Tyree MT (1990) Water-stress-induced xylem embolism in three species of conifers. **Plant Cell Environ** 13: 427–436

Sperry JS, Venturas MD, Anderegg WR, Mencuccini M, Mackay DS, Wang Y, Love DM (2017) Predicting stomatal responses to the environment from the optimization of photosynthetic gain and hydraulic cost. **Plant Cell Environ** 40: 816–830

Sperry JS, Wang Y, Wolfe B, Mackay DS, Anderegg WRL, McDowell NG, Pockman WT (2016) Pragmatic hydraulic theory predicts stomatal responses to climatic water deficits. **New Phytol** 212: 577–589

Stanfield RC, Hacke UG, Laur J (2017) Are phloem sieve tubes leaky conduits supported by numerous aquaporins? **Am J Bot**. 104: 719–732

Steinberg S, van Bavel CH, McFarland MJ (1989) A gauge to measure mass flow rate of sap in stems and trunks of woody plants. **J Am Soc Hort Sci** 114: 466–472

Steudle E (2000) Water uptake by plant roots: An integration of views. **Plant Soil** 226: 45–56

Stiller V, Sperry JS (2002) Cavitation fatigue and its reversal in intact sunflower plants. **J Exp Bot** 53: 1155–1161

Tai X, Mackay DS, Anderegg WR, Sperry JS, Brooks PD (2017) Plant hydraulics improves and topography mediates prediction of aspen mortality in southwestern USA. **New Phytol** 213: 113–127

Taiz L, Zeiger E (2010) Water balance of plants. In: Taiz L, Zeiger E, ed. *Plant Physiology*. Fifth. Sinauer Associates, Sunderland, Massachusetts, USA. pp. 85–105

Taylor-Laine SD, Espino S, Downey A, Schenk HJ (2016) Testing a new method for in situ measurements of stem hydraulic conductance in intact plants. ICT International, Armidale, New South Wales, Australia. pp. 1–5. www.ictinternational.com

Tobin MF, Pratt RB, Jacobsen AL, De Guzman ME (2013) Xylem vulnerability to cavitation can be accurately characterised in species with long vessels using a centrifuge method. **Plant Biol** 15: 496–504

Torres-Ruiz JM, Jansen S, Choat B, McElrone AJ, Cochard H, Brodribb TJ, Badel E, Burlett R, Bouche PS, Brodersen CR (2015) Direct X-ray microtomography observation confirms the induction of embolism upon xylem cutting under tension. **Plant Physiol** 167: 40–43

Torres-Ruiz JM, Cochard H, Mencuccini M, Delzon S, Badel E (2016) Direct observation and modelling of embolism spread between xylem conduits: A case study in Scots pine. **Plant Cell Environ** 39: 2774–2785

Torres-Ruiz JM, Sperry JS, Fernández JE (2012) Improving xylem hydraulic conductivity measurements by correcting the error caused by passive water uptake. **Physiol Plant** 146: 129–135

Tötzke C, Miranda T, Konrad W, Gout J, Kardjilov N, Dawson M, Manke I, Roth-Nebelsick A (2013) Visualization of embolism formation in the xylem of liana stems using neutron radiography. **Ann Bot** 111: 723–730

Trifilò P, Raimondo F, Lo Gullo MA, Barbera PM, Salleo S, Nardini A (2014) Relax and refill: xylem rehydration prior to hydraulic measurements favours embolism repair in stems and generates artificially low PLC values. **Plant Cell Environ** 37: 2491–2499

Tsuda M, Tyree MT (1997) Whole-plant hydraulic resistance and vulnerability segmentation in *Acer saccharinum*. **Tree Physiol** 17: 351–357

Tuberosa R, Salvi S (2006) Genomics-based approaches to improve drought tolerance of crops. **Trends Plant Sci** 11: 405–412

Tyree MT (1997) The cohesion-tension theory of sap ascent: Current controversies. **J Exp Bot** 48: 1753–1765

Tyree MT, Alexander J, Machado JL (1992) Loss of hydraulic conductivity due to water stress in intact juveniles of *Quercus rubra* and *Populus deltoides*. **Tree Physiol** 10: 411–415

Tyree MT, Cochard H, Cruiziat P, Sinclair B, Ameglio T (1993) Drought-induced leaf shedding in walnut: Evidence for vulnerability segmentation. **Plant Cell Environ** 16: 879–882

Tyree MT, Dixon MA, Tyree EL, Johnson R (1984) Ultrasonic acoustic emissions from the sapwood of cedar and hemlock: An examination of three hypotheses regarding cavitations. **Plant Physiol** 75: 988–992

Tyree MT, Patino S, Bennink J, Alexander J (1995) Dynamic measurements of root hydraulic conductance using a high-pressure flowmeter in the laboratory and field. **J Exp Bot** 46: 83–94

Tyree MT, Salleo S, Nardini A, Lo Gullo MA, Mosca R (1999) Refilling of embolized vessels in young stems of laurel. Do we need a new paradigm? **Plant Physiol** 102: 11–21

Tyree MT, Sperry JS (1988) Do woody plants operate near the point of catastrophic xylem dysfunction caused by dynamic water stress? Answers from a model. **Plant Physiol** 88: 574–580

Urban J, Dvořák M (2014) Sap flow-based quantitative indication of progression of Dutch elm disease after inoculation with *Ophiostoma novo-ulmi*. **Trees** 28: 1599–1605

Utsumi Y, Sano Y, Funada R, Fujikawa S, Ohtani J (1999) The progression of cavitation in earlywood vessels of *Fraxinus mandshurica* var *japonica* during freezing and thawing. **Plant Physiol** 121: 897–904

Utsuzawa S, Fukuda K, Sakaue D (2005) Use of magnetic resonance microscopy for the nondestructive observation of xylem cavitation caused by pine wilt disease. **Phytopathology** 95: 737–743

van Bel AJ (2003) The phloem, a miracle of ingenuity. **Plant Cell Environ** 26: 125–149

Vargaftik N, Volkov B, Voljak L (1983) International tables of the surface tension of water. **J Phys Chem Ref Data** 12: 817–820

Venturas MD, López R, Martín J, Gascó A, Gil L (2014) Heritability of *Ulmus minor* resistance to Dutch elm disease and its relationship to vessel size, but not to xylem vulnerability to drought. **Plant Pathol** 63: 500–509

Venturas MD, MacKinnon ED, Dario HL, Jacobsen AL, Pratt RB, Davis SD (2016a) Chaparral shrub hydraulic traits, size, and life history types relate to species mortality during California's historic drought of 2014. **PLoS ONE** 11: e0159145

Venturas MD, MacKinnon ED, Jacobsen AL, Pratt RB (2015) Excising stem samples underwater at native tension does not induce xylem cavitation. **Plant Cell Environ** 38: 1060–1068

Venturas MD, Rodriguez-Zaccaro FD, Percolla MI, Crous CJ, Jacobsen AL, Pratt RB (2016b) Single vessel air injection estimates of xylem resistance to cavitation are affected by vessel network characteristics and sample length. **Tree Physiol** 36: 1247–1259

Vesala T, Holtta T, Peramaki M, Nikinmaa E (2003) Refilling of a hydraulically isolated embolized xylem vessel: Model calculations. **Ann Bot** 91: 419–428

Wang R, Zhang L, Zhang S, Cai J, Tyree MT (2014) Water relations of *Robinia pseudoacacia* L.: Do vessels cavitate and refill diurnally or are R-shaped curves invalid in Robinia? **Plant Cell Environ** 37: 2667–2678

Wang Z, Wang CY, Fang ZM, Zhang DL, Liu L, Lee MR, Li Z, Li JJ, Sung CK (2010) Advances in research of pathogenic mechanism of pine wilt disease. **Afr J Microbiol Res** 4: 437–442

West AG, Nel JA, Bond WJ, Midgley JJ (2016) Experimental evidence for heat plume-induced cavitation and xylem deformation as a mechanism of rapid post-fire tree mortality. **New Phytol** 211: 828–838

Wheeler JK, Huggett B, Tofte A, Fulton R, Holbrook NM (2013) Cutting xylem under tension or supersaturated with gas can generate PLC and the appearance of rapid recovery from embolism. **Plant Cell Environ** 36: 1938–1949

Wheeler JK, Sperry JS, Hacke UG, Hoang N (2005) Inter-vessel pitting and cavitation in woody Rosaceae and other vesselled plants: A basis for a safety vs. efficiency trade-off in xylem transport. **Plant Cell Environ** 28: 800–812

Wheeler TD, Stroock AD (2008) The transpiration of water at negative pressures in a synthetic tree. **Nature** 455: 208–212

Wolf A, Anderegg WRL, S.W. P (2016) Optimal stomatal behavior with competition for water and risk of hydraulic impairment. **Proc Natl Acad Sci USA** 113: E7222–E7230

Wolfe B, Sperry JS, Kursar T (2016) Does leaf shedding protect stems from cavitation during seasonal droughts? A test of the hydraulic fuse hypothesis. **New Phytol** 212: 1007–1018

Wortemann R, Herbette S, Barigah TS, Fumanal B, Alia R, Ducousso A, Gomory D, Roeckel-Drevet P, Cochard H (2011) Genotypic variability and phenotypic plasticity of cavitation resistance in *Fagus sylvatica* L. across Europe. **Tree Physiol** 31: 1175–1182

Wullschleger SD, Meinzer FC, Vertessy RA (1998) A review of whole-plant water use studies in trees. **Tree Physiol** 18: 499–512

Yang S, Tyree MT (1992) A theoretical model of hydraulic conductivity recovery from embolism with comparison to experimental data on *Acer saccharum*. **Plant Cell Environ** 15: 633–643

Yang S, Tyree MT (1993) Hydraulic resistance in *Acer saccharum* shoots and its influence on leaf water potential and transpiration. **Tree Physiol** 12: 231–242

Yang S, Tyree MT (1994) Hydraulic architecture of *Acer saccharum* and *A. rubrum*: Comparison of branches to whole trees and the contribution of leaves to hydraulic resistance. **J Exp Bot** 45: 179–186

Yang SJ, Zhang YJ, Sun M, Goldstein G, Cao KF (2012) Recovery of diurnal depression of leaf hydraulic conductance in a subtropical woody bamboo species: Embolism refilling by nocturnal root pressure. **Tree Physiol** 32: 414–422

Zheng Q, Durben DJ, Wolf GH, Angell CA (1991) Liquids at large negative pressures: Water at the homogeneous nucleation limit. **Science** 254: 829–832

Zimmermann MH (1978) Hydraulic architecture of some diffuse porous trees. **Can J Bot** 56: 2286–2295

Zimmermann MH (1983) *Xylem Structure and the Ascent of Sap*. Springer, Berlin Heidelberg New York

Zimmermann U, Schneider H, Wegner L, Haase A (2004) Water ascent in tall trees: Does evolution of land plants rely on a highly metastable state? **New Phytol** 162: 575–615

Zwieniecki MA, Holbrook NM (2000) Bordered pit structure and vessel wall surface properties. Implications for embolism repair. **Plant Physiol** 123: 1015–1020

Zwieniecki MA, Melcher PJ, Holbrook NM (2001) Hydrogel control of xylem hydraulic resistance in plants. **Science** 291: 1059–1062